BEHAVIOUR OF REINFORCED CONCRETE CYLINDRICAL SHELL WITH TIE BARS

BY

PRIYAVADAN N. MEHTA

DEPARTMENT OF CIVIL ENGINEERING

INDIAN INSTITUTE OF TECHNOLOGY KANPUR

SEPTEMBER 1969

BEHAVIOUR OF REINFORCED CONCRETE CYLINDRICAL SHELL WITH TIE BARS

Thesis Submitted in Partial Fulfilment
of the Requirements for the
Degree of

MASTER OF TECHNOLOGY

in

CIVIL ENGINEERING

by

PRIYAVADAN N. MEHTA

DEPARTMENT OF CIVIL ENGINEERING
INDIAN INSTITUTE OF TECHNOLOGY, KANPUR

September 1969

CERTIFICATE

The thesis on "Behaviour of Reinforced Concrete Cylindrical Shell with Tie Bars" by Mr. P. N. Mehta, as a partial fulfilment towards the degree of Master of Technology in Civil Engineering is accepted.

P Dayaratnam

(P. Dayaratnam)
Associate Professor
and Chairman of Thesis Committee

Kanpur,
September 1969

ACKNOWLEDGEMENTS

The writer expresses his deep sense of gratitude to Dr. P. Dayaratnam for suggesting this problem and giving valuable guidance throughout this research work. The writer is thankful to Mr. S.C. Goel and Mr. Hark Singh for their cooperation in experimental work.

ABSTRACT

The cylindrical shells are designed in several combinations of the longitudinal edge directions. Some of the common edge conditions are (1) Free Edges, (2) Longitudinal Edge Beams, (3) Continuous Barrel Types, (4) Transverse Tie Bars with or without Edge Beams, and (5) Transverse Diaphragms. Sometime these shells are constructed continuous over the transverse supports. Many times, it is not obvious what type of edge conditions would yield an economical solution. The present investigation is aimed at a very specific optimal problem of the shell construction. The optimal problem referred here is associated with the need and design of transverse tie bars based on behavioural aspect rather than cost. The object of the investigation is to seek the rational solutions to the following questions.

1. What type of shells need to be provided with transverse tie bars?

2. If a shell is provided with the tie bars, then,

(a) What should be the area of cross-section of the tie bars?

(b) What is the effect of the spacing of the tie bars on the flexural behaviour and ultimate strength of the shell?

(c) What is the cracking pattern of the shell with respect to the spacing of the tie bars?

(d) How does the stiffness and the strength of a cylindrical shell compare with that of a folded plate with similar dimensions and tie bars?

(e) Is it possible to idealise a concentrated load on the shell as a distributed load based on virtual work concept and to predict reasonable deformations or stress resultants for the concentrated load?

(f) What are the secondary effects in the region of the tie bar?

3. If a flexural crack is produced in a shell, is it possible to dampen the crack propagation with the help of the tie bars?

The solutions to these problems were sought through experimental and analytical methods. An identical set of microconcrete cylindrical shells were tested under two point loads. Each shell was tested with different spacings of the tie bars for its elastic

behaviour and then loaded to its ultimate capacity for a particular spacing of the tie bars. Three specimens were tested for any given spacing of the tie bars. These specimens have given very consistent results.

One shell without tie bars which developed a flexural crack in the longitudinal beam was unloaded and then provided with tie bars at the cracked location. Then this shell was tested for its behaviour after providing the tie bars.

The point loads were idealised as distributed load based on virtual work concept. The shell is then analyzed by a Schorer Theory and the deformations measured from the experimental work were compared with the analytical results.

A cylindrical shell subjected to uniformly distributed vertical load over the surface will deflect vertically downward without horizontal displacement under membrane state. The shells normally adopted in the civil engineering construction have the included angles more than 50°. If these shells are designed with free longitudinal edges, then the free edges have the tendency to deflect inwards. Provision of the tie bars in such shells is not of much use, whereas intermediate diaphragms are more helpful in keeping the

shape of the shells. In case of shells with edge beams, if the flexural stiffness of the edge beams in the vertical plane is very high, then the shell will have a flattening tendency. The transverse tie bars in such shells are helpful. If the longitudinal edges of the shells are supported by rigid walls, then flattening action is dominant and the need for tie bars is high.

The vertical deflections of the shells observed from the experimental results decrease with decrease in the spacing of the transverse tie bars. However, the rate of decrease in the deflection reduces and becomes asymptotic for a spacing of about 2/3 of the chord width. It is recommended that the spacing of the tie bars be adopted equal to the chord width as further decrease in the deformation beyond this spacing is of small magnitude. The ultimate capacity of the shells increased with decrease in the spacing of the tie bars. The tie bar force was measured by electrical strain gauges and found to be of small magnitude. The total force in the tie bars varied from 6 to 15 percent of the vertical load acting on the shell. This amount of force is not very much since the tie bars are under direct tension. The tie bars are recommended to be designed for about 15 percent of the vertical load. The crack pattern of the shell at ultimate load changed with change

in the spacing of the tie bars. The number of the cracks developed, increased with increase in the number of the tie bars. The more number of small cracks might have contributed towards the increase in the ultimate capacity of the shells with small tie bar spacings.

It is probably obvious that the cylindrical shell is much stiffer than a folded plate of similar dimensions under distributed load conditions. The cylindrical shell was found to be much stiffer than the folded plate with respect to even concentrated loads on the crown or ridge of the structures. The two concentrated loads acting on the shell were idealised as uniformly distributed load based on virtual work concept. The vertical deflections predicted by using the Schorer Theory for the equivalent distributed load were then compared with the experimental results and found to give reasonable results. However, the horizontal deflections did not check well. The shells were instrumented with strain gauges and linear deflection dial gauges. The data obtained from this instrumentation was not enough to study the secondary effects of the tie bars on the shell. However, the overall behaviour of the shell did not indicate any deteriorating effects due to the tie bars. The shell that had developed flexural cracks in the edge beams when again tested with

tie bars at the cracked locations, gave an improved performance. The initial cracks did not propagate, in fact, they got closed with the provision of the tie bar.

Considerable research work has been done on the cylindrical shell. However, most of this work is based towards analysis oriented. There is a great need for further research on the optimal design aspect of the shells. What is discussed in this investigation is very small as compared to the work that is to be done in the direction of the design. An overall optimization with respect to the geometry (that is rise, chord and length relations), the edge conditions (that the edge beams and their relation to the shell), continuity and intermediate diaphragm conditions should be done. The designer or the field engineer should be provided with certain guide lines in making appropriate parameter choices and decisions. The present investigation has discussed a specific load condition to establish certain qualitative data associated with the cylindrical shells. It is highly desirable to study the optimization problem for self-weight and wind or live load conditions. Looking at the designer's point of view, there is much more to be done even in the field of optimal design of the cylindrical shells.

CONTENTS

NOTATIONS

A - Area

A_s - Area of Steel

B - Chord Width

CSO - Cylindrical Shell with No Tie Bar

CS1 - Cylindrical Shell with One Tie Bar

CS2 - Cylindrical Shell with Two Tie Bars

CS3 - Cylindrical Shell with Three Tie Bars

CS4 - Cylindrical Shell with Four Tie Bars

CS5 - Cylindrical Shell with Five Tie Bars

E_c - Modulus of Elasticity of Concrete

E_s - Modulus of Elasticity of Mild Steel

E_T - Modulus of Elasticity of High Strength Steel

FPO - Folded Plate with No Tie Bar

FP1 - Folded Plate with One Tie Bar

f'_c - Cylinder Strength of Concrete

f_y - Yield Stress of Mild Steel

KSC - Kgs/cm^2

L - Span of Shell

L_t - Length of Tie Bar

M_ϕ - Transverse Moment

N_ϕ - Transverse Axial Force

$N_{x\phi}$ - In-plane Shear Force

Q_ϕ - Transverse Shear Force

R - Radius

s - Spacing of Tie Bars

T - Tie Force

t - Thickness of Shell

u - Longitudinal Displacement

v - Transverse Displacement

w - Radial Displacement

ϕ - Angle

ϕ_c - Semi-central Angle

ϑ - Rotation

w_d - Uniform Load

CHAPTER I

INTRODUCTION

1.1 Brief Review of Literature

The simplest form of the curved roof commonly employed for industrial buildings is cylindrical shell. It has been studied in great length both theoretically and experimentally. A brief review of the work done on the cylindrical shell is discussed in the present section. The theories for the Analysis of the Shell are not discussed in the review.

The experiments on the models of eleven shells made from Reinforced and Prestressed Concrete were carried by A.L. Bouma* (1) et al. A series of seven shells was taken with a particular view. The amount of reinforcement in the edge beams of the series was kept constant, but its distribution was varied. Another two reinforced concrete shells with different lengths were taken in order to study the influence of length. The remaining two shells were a reinforced concrete shell on continuous supports and a prestressed concrete shell. As regards the loading, a number of point loads were applied on all eleven models. All the shells were

*The number in parenthesis indicates the reference number.

loaded up to failure.

The experiments of the series consisting of seven shells provided good information about the failure mechanism. The shell which had practically no reinforcement in the shell portion, failed suddenly and catastrophically. The shell with uniform reinforcement provided over entire depth of edge beam yielded at a lower load than that of shell with the reinforcement being dumped as low as possible. It was observed that the shell designed in a traditional way behaved satisfactorily in every respect.

The reinforcement in continuous reinforced concrete shell yielded at a higher load compared to that of any shell from the series. The yield load of the reinforcement in Prestressed Concrete Shell was maximum among all the cases.

The introduction of edge beams decreases the stresses. The variation of the stresses tends to the linearity. In this regards, the effect of edge beams with different shapes and sizes on the stresses in the shell, was studied by Dr. A.S. Arya (2) and Mr. S.K. Agarwal. Holland and Schorer theories were adopted to study the problem. The short, intermediate and long shells with edge beams being varied in shape and size were analyzed.

The stresses obtained from Schorer Theory were close to the stresses obtained from Holland Theory, in the case of Intermediate and Long Shells. But, Schorer Theory results deviated largely from Holland Theory results in the case of Short Shells.

The transverse moment in the case of flat edge beams was more than that in the case of deep edge beams. The twisting moment increased in the case of flat edge beams. The longitudinal and transverse axial forces, and shear forces in the shell with deep edge beams were less compared to those in the shell with flat edge beams. The results had made conclusion that the narrow deep edge beam was generally superior to all other shapes, for all the shells.

A Reinforced Mortar Model of Parabolic Cylindrical Shell with variable thickness was tested by Arthur W. Hedgren, Jr. (3) and David P. Billington. The vacuum loading was applied on the shell. In consequence of this, the normal loading was developed. This resulted more deflection at the edge than that at the crown. At the higher load, the crown was lifted upwards.

The experimental deflections, stresses, moments were close to the corresponding theoretical results within elastic range. At higher loads, the experimental deflections, stresses, moments were considerably higher than corresponding theoretical results.

The first cracking was developed in the corners of the shell and continued to propagate towards the centre as the load was further increased. At high loads, the longitudinal cracks showing the yielding of transverse reinforcement had developed at the crown. At the failure load, the diagonal cracks and longitudinal cracks were combined. So, the ultimate load carrying capacity was governed by the transverse flexural strength and shear.

The influence of Prestressing on stresses in the single cylindrical shells was theoretically studied by M.L. Kalra (4). The Finsterwalder Theory was applied to analyze the shell. It was found that the transverse moment had increased due to the prestress. The shell was found to deflect outward and it continued to deflect more as the prestressing was increased. To restrain this displacement, the author had introduced the transverse tie bars with certain spacing at springing line. It was found that the transverse moment ceased to increase at the same rate as was in the case of no tie bar. Horizontal displacement was considerably decreased.

1.2 Proposed Investigation

Much work has been done on the cylindrical shell. But, the effect of transverse tie bars being varied in number and spacing is not studied. The tie bars are of

much concern in single shells and the exterior bays of multiple shells. The need to provide tie bars in the exterior bays of multiple shells is explained in Fig. 1.1.

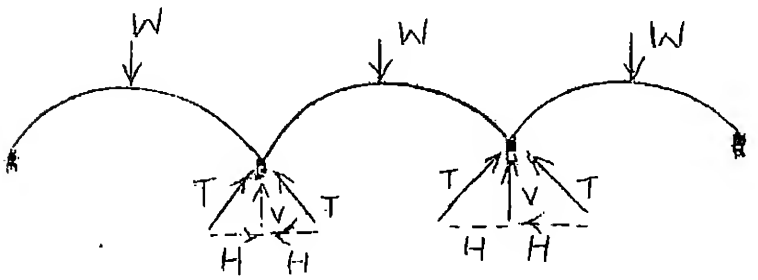

Fig. 1.1 The Reactions in Multiple Shells

The reactions in multiple shells are shown in the Fig. 1.1. The horizontal components of the edge thrusts at the junction of the two adjacent shells are compensating. Therefore, the intermediate longitudinal beams are subjected to the vertical loads. The outer edge beams of the exterior bays unless restrained by an external or support hinge, are free to deform and move in the horizontal direction.

The need of the tie bars in a single shell with free edges does not require any further explanation.

If the horizontal movement is restrained, the stresses in the shell might get reduced. In consequence

of this, a thinner section can be adopted and the amount of reinforcement would be reduced.

The restraint may be introduced through intermediate diaphragms or transverse tie bars. Keeping the construction view in mind, the introduction of the tie bars would be easier compared to the provision of the diaphragms. And, the tie bars may roughly fulfil the same structural benefit produced by diaphragms.

The present investigation was carried out with the following objectives.

Objectives

1. To find the behaviour of cylindrical shell with transverse tie bars.

2. To find an optimum spacing and area of the tie bars.

3. To compare the stiffness of the cylindrical shell with that of the folded plate of similar dimensions.

4. To compare the experimental results with the theoretical results in the elastic range.

5. To make some recommendations when a tie bar is needed with reference to the shell included angle, edge beam etc.

A set of five long micro-concrete circular cylindrical shells with the tie bars were tested for the flexural behaviour. The experimental results were compared with the results obtained from Schorer and Beam Theories.

CHAPTER II

EXPERIMENTAL WORK

2.1 Materials

Microconcrete was used for cylindrical shells under investigation. The properties of the materials used in the specimens are discussed in the following section.

Ordinary portland cement exhibiting standard qualities was used. The river sand with the specific gravity of 2.5 was used as fine aggregate. The coarse aggregate with the fineness modulus of 6.5 was of hard granite.

Mild steel bars of 9.4 mm dia. were used as longitudinal reinforcement in the edge beams. Fig. 2.1 gives the stress-strain behaviour of the bars. Mild steel wires of 3.2 mm, spaced at 80 mm, were used in the longitudinal and transverse directions of the shell. The high strength steel bar of 7 mm dia. was used as the Tie Bar. Fig. 2.2 gives the stress-strain behaviour of the high strength steel bar.

2.2 Specimens

A teak wood mould was used for casting of the cylindrical shell specimens. The top of the mould was fixed with a G.I. sheet. This type of fixing of the

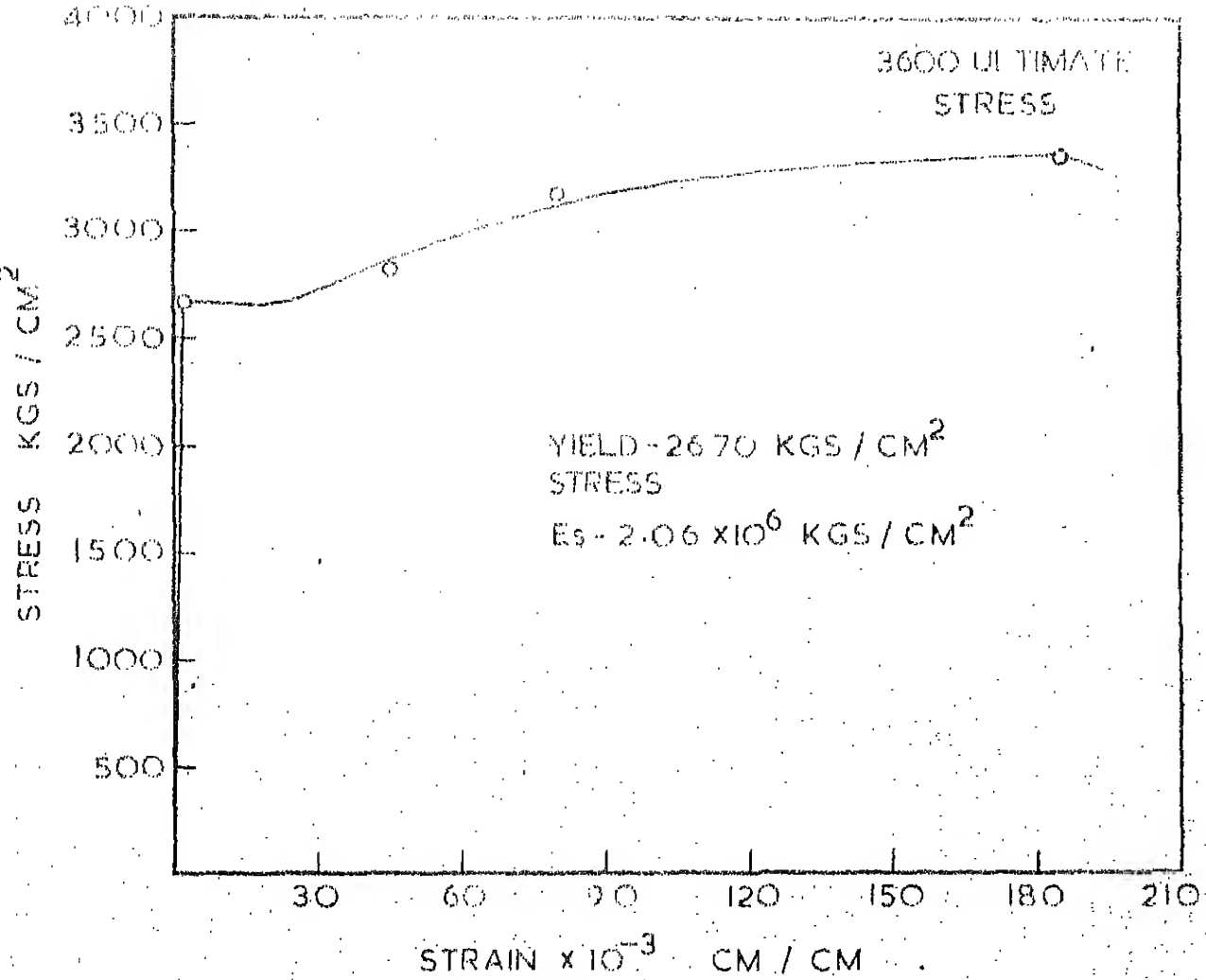

FIG. 2·1 STRESS – STRAIN CURVE FOR M. S.

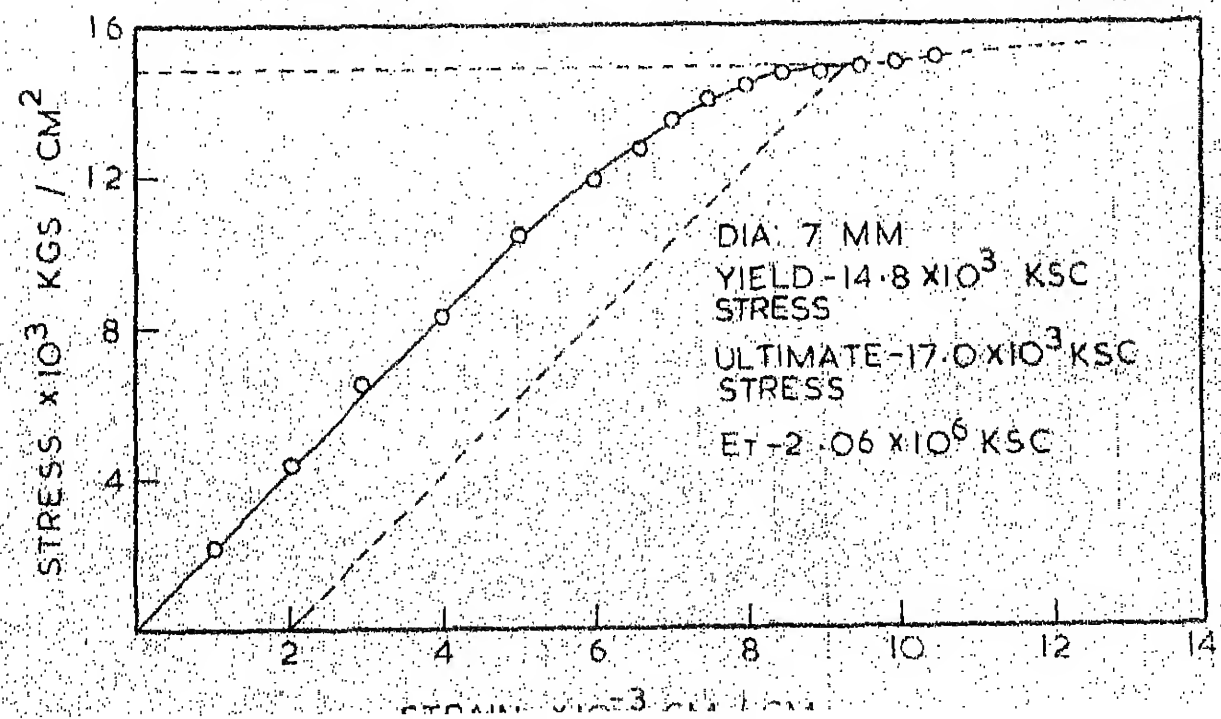

sheet avoids absorption of water by the mould from wet concrete and also gives a much better finishing to the specimen.

2.2.1 Specimens

The five micro-cement concrete shells with reinforcement were cast for the testing. The salient features of the geometry of the shell are shown in Fig. 2.3.

The diaphragms at the junction were tappered to facilitate the separation of the specimen from the mould.

Two specimens were cast without any provision for the tie bars. These two specimens were tested for behaviour of the shell without the tie bars. Three specimens were provided with five holes at the junction of the shell and edge beams. The holes for the tie bars are spaced at 250 mm along the length of the shell. The provision of five holes facilitates to vary the number of the tie bars.

The specimen view is shown in Photograph : 1.

2.2.2 Preliminary Design Aspect

The shell with the edge beams behaves like a beam, in the case of Span/Radius ≥ 3. The shell under

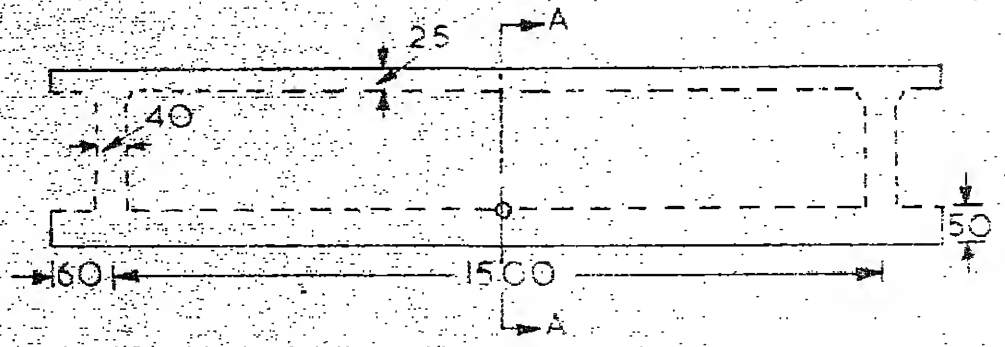

ELEVATION

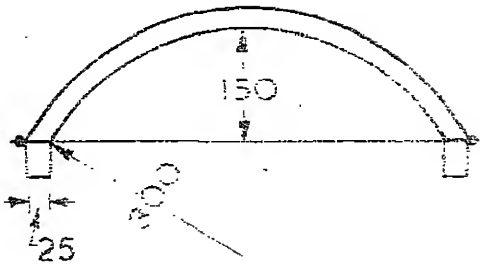

END VIEW (SECTION A-A)

FIG. 2·3 DETAILS OF THE SHELL

ALL DIMENSIONS IN MM

was designed like a beam with curved cross-section. The amount of longitudinal reinforcement is found on the basis of Working Stress Design which is shown in Appendix A-1.

The force in the tie bar is determined by Arch Method. The Arch is assumed to be hinged at two edges. The method to find out the tie bar force and subsequently area of tie bar is illustrated in Appendix A-2.

2.2.3 Details of Reinforcement Layout

Two bars of 9.4 mm were placed in each of the edge beams. The ends of the bars were kept beyond the diaphragms, in order to achieve the anchorage length. The wires of 3.2 mm spaced at 80 mm, were provided in longitudinal and transverse directions of the shell for shrinkage and temperature stresses. The transverse wires would also function to resist negative transverse moment. The diaphragms were vertically reinforced. Good bond was developed between diaphragm and shell reinforcement being tied to each other. Shear reinforcement of the same wire was diagonally provided near the support to avoid shear cracking.

The details of reinforcement layout are shown in Fig. 2.4. The reinforcement of the shell is shown in Photograph: 2.

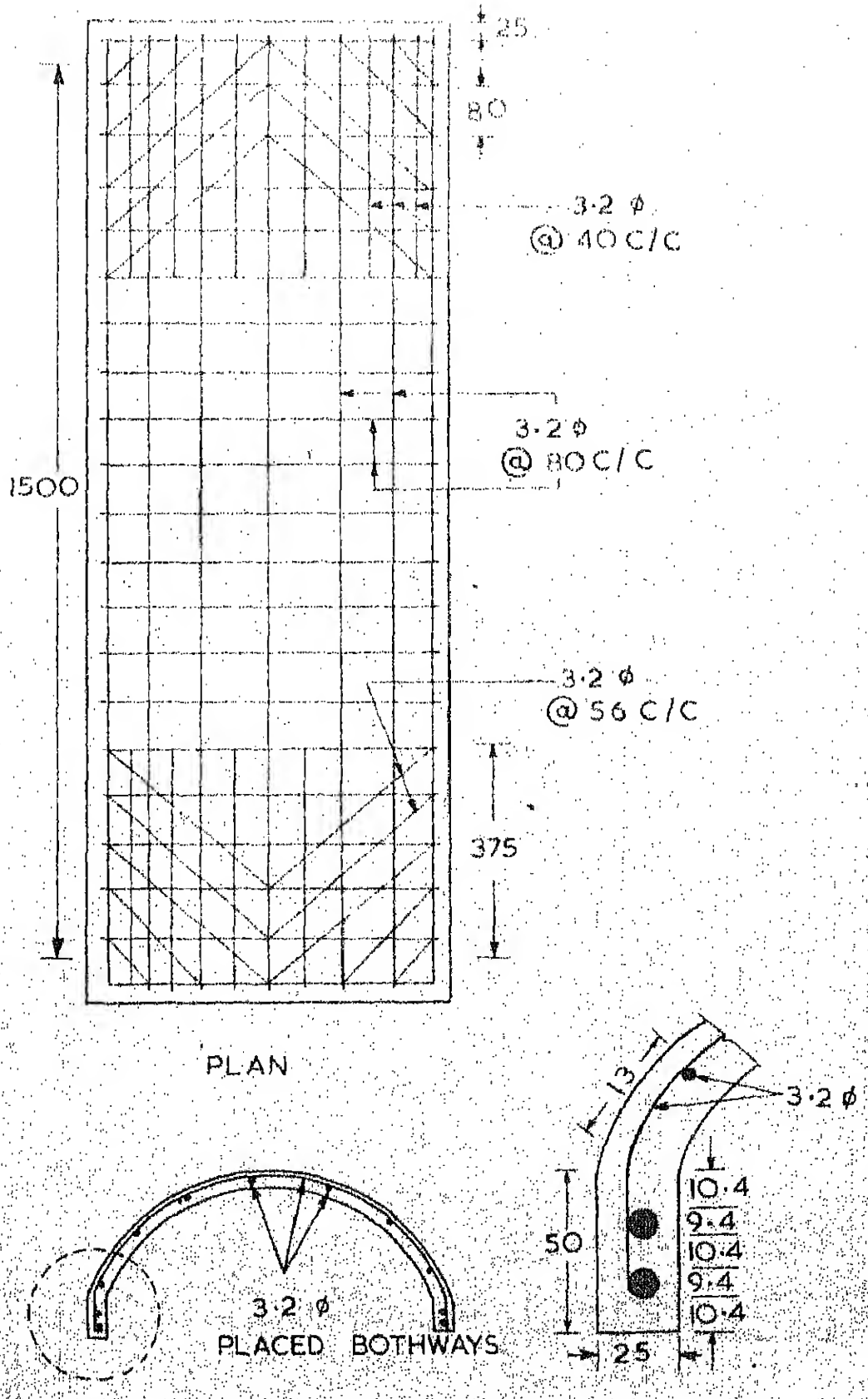

FIG. 2·4 REINFORCEMENT DETAILS
(ALL DIMENSIONS IN M M)

2.2.4 Casting and Curing

All the micro-concrete shells were cast with 1:1:2 mix by weight. The W/C ratio by weight was to be 0.45.

The mix was prepared in Tilting Mixer having 0.028 cu-metres capacity. The prepared mix was spread over the mould. It was externally vibrated. Care was taken not to allow the air-voids in the edge beams. All the shells were cured in water-pond for 30 days.

2.3 Experimental Set-up

All the specimens were tested on the self-straining loading frame as shown in Fig. 2.5. The I-section was kept over two channels, each connected to a column. The rod working as a roller was placed between the channel section and the I-section. The function of the rod was to transmit the load to the web of the channel section, so that the yielding of the support would practically be zero.

The diaphragms were resting over the webs of the I-section through rollers. One end of the specimen was not allowed to move. While, another end was allowed to do so.

The experimental set-up is shown in Photograph: 3.

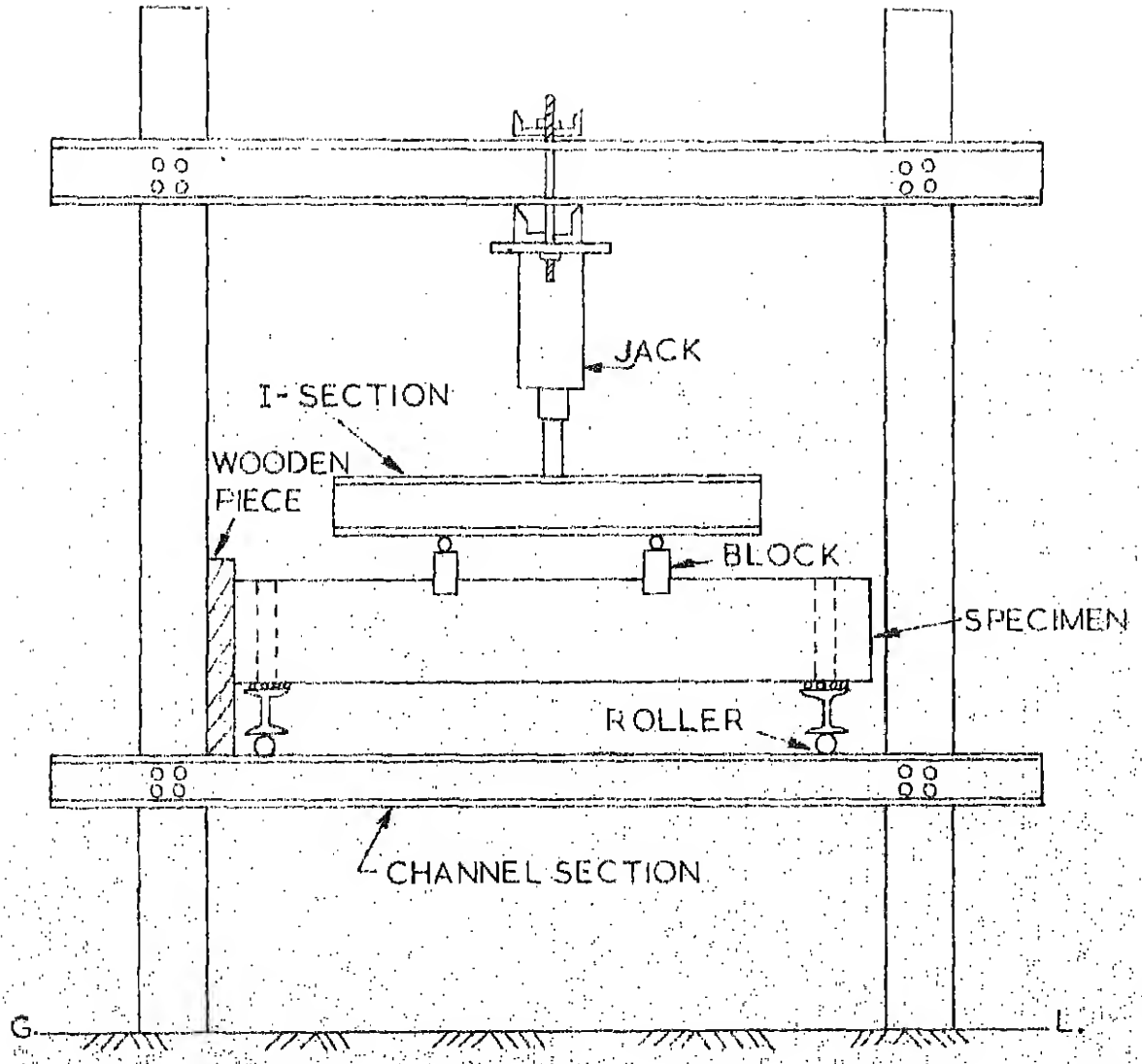

FIG. 2·5 LOADING FRAME

Loading

The effect of the tie bars in pure flexure was the main object of the programme. It was also aimed to compare the stiffness of the cylindrical shell having the tie bars with that of the folded plate having the tie bars. The loading on the folded plate was a two point load. So, to be consistent with the loading on the folded plate, the same form of the loading was applied on the cylindrical shell. This type of loading is an idealised form for study of flexural behaviour as a starting point.

Two equal point loads, each at L/3 from the support, were applied on the specimen to create pure moment area through middle-third portion. The two point load was achieved through two segmental blocks which rest on the ridge of the shell. A layer of the Plaster of Paris was placed in between the block and the upper surface of the shell. This helped in preventing the crushing of the concrete. The loading was developed by hydraulic jack.

2.4 Instrumentation

2.4.1 Set-up of the Dial Gauges

Fig. 2.6 illustrates the arrangement of dial gauges placed on the specimen. The gauges were mounted

from the frame made from the slotted angles. The least count of the dial gauge placed on the shell was 0.01 mm, while that of the dial gauge placed under the support was 0.002 mm.

Four kinds of deflections were measured. As shown in Fig. 2.6, the gauges placed along L-1, O-1, R-1 lines were showing the radial deflections. The gauges placed under the edge beam measured vertical deflections. The gauges placed at centre-line of edge beams were indicating horizontal displacements. The gauges placed under the support were kept to measure the yielding of the support.

2.4.2 Set-up of Strain-Gauges

The electrical strain-gauge was used to measure the strain. SR-4 strain gauge was adopted. The four-arm Wheatstone Bridge Circuit was used to measure the strains. Its gauge factor was 1.98. A body exhibiting the same properties of the specimen was fixed with strain gauge to compensate the temperature stresses.

Two strain gauges were fixed on diametrically opposite faces of the tie bar. The average of two measurements was considered to determine the force in the tie bar

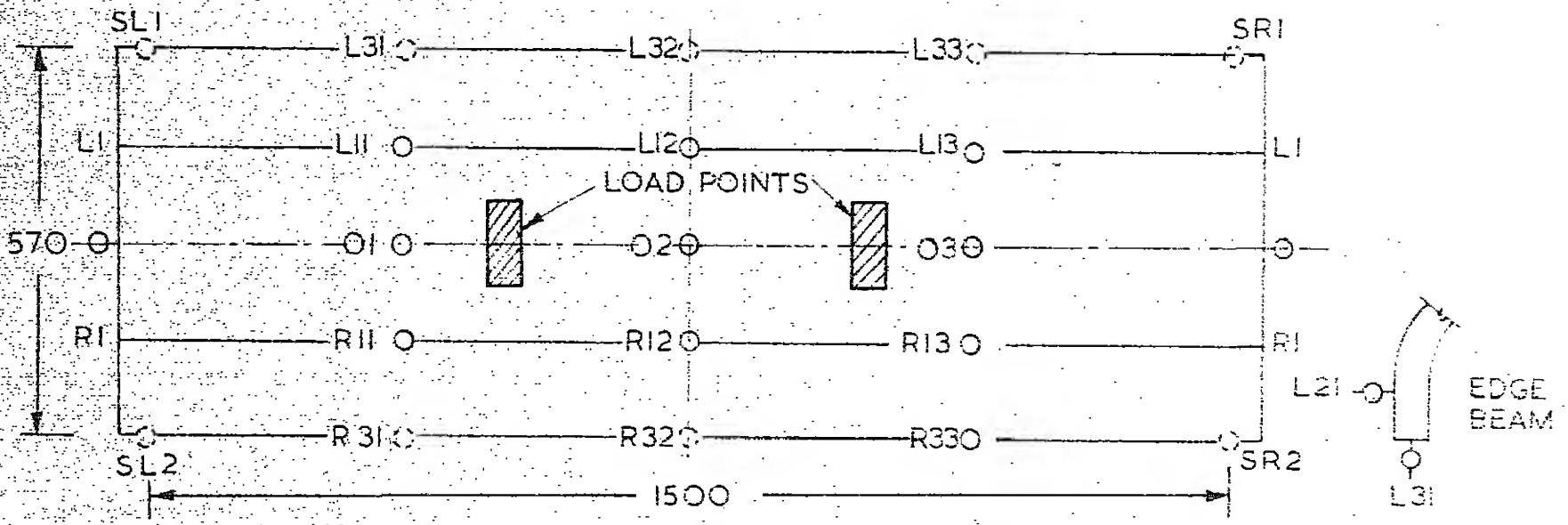

FIG. 2·6 LAY OUT OF DIAL GAUGES

ALL DIMENSIONS IN MM

LINE	POSITION OF DIAL GAUGES
O - O R1 - R1 L1 - L1	RADIALLY
R2 - R2 L2 - L2	HORIZONTALLY
R3 - R3 L3 - L3	VERTICALLY

2.5 Testing of the Specimens

The variable parameter in the study is spacing of the tie bars. Two shells without the tie bars were tested up to failure. Three shells were tested with the tie bars being varied in spacing. Three shells with one tie, two tie bars and three tie bars respectively were tested up to failure. Each of the last three shells was tested for five cases of tie bars positioned as shown in Fig. 2.7, up to elastic range.

The notations CS0, CS1 indicate the cylindrical shells with no and one tie bar respectively. The same argument follows the notations CS2, CS3, CS4, CS5.

The instrumentation was the same for all the specimens.

Cube Strength

The concrete cubes were tested on the same day of the specimen testing. The cube strengths of five shells are given in Table 2.1.

Specimen Number	Average Strength of Three Cubes in Kgs/cm^2
I	471.1
II	397.9
III	376.1
IV	398.7
V	488.7

Table 2.1
Cube Strength

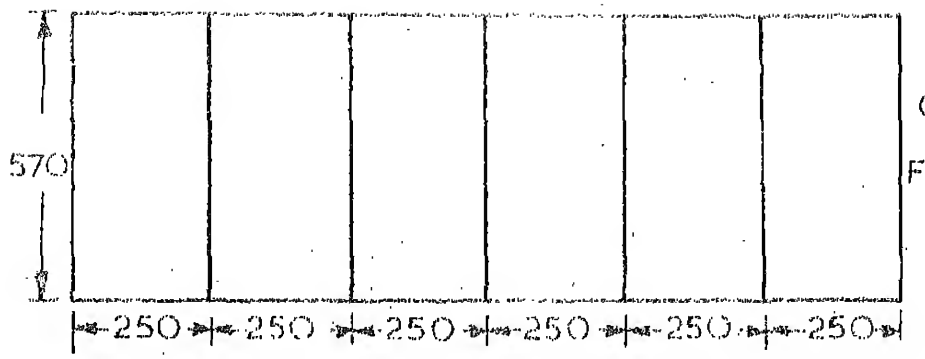

CS 5

FIVE TIE BAR

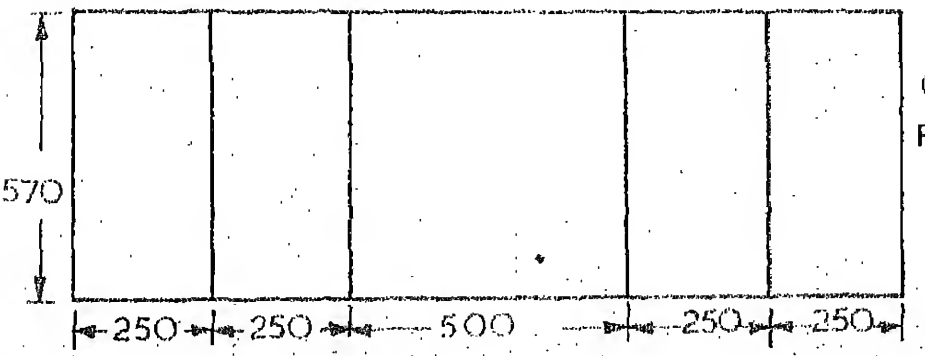

CS 4

FOUR TIE BA

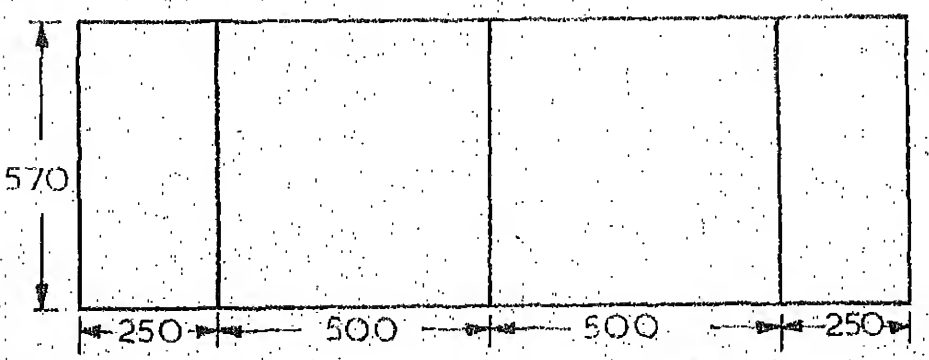

CS 3

THREE TIE B

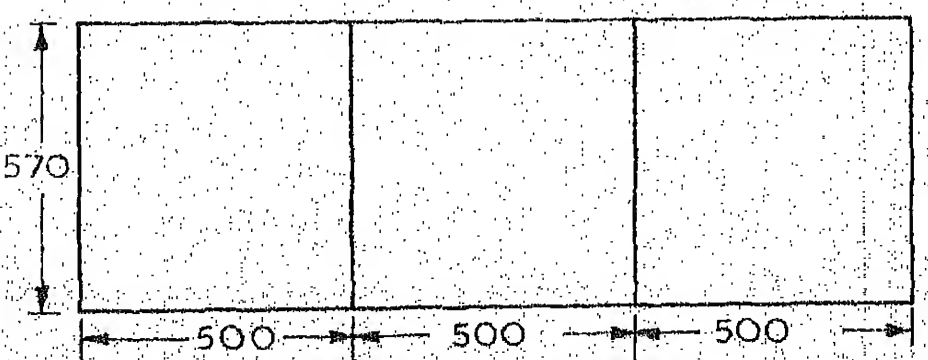

CS 2

TWO TIE BA

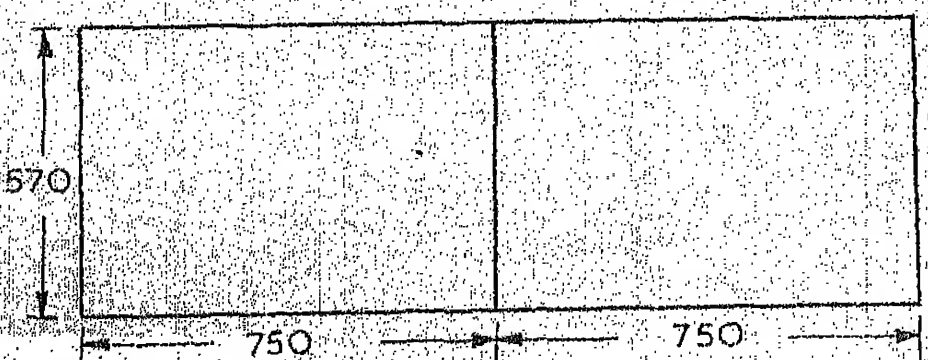

CS 1

ONE TIE BA

The average strength is found to be 413.6 kgs/cm^2. All the cube strengths are within the range of $\pm$ 12% of the average value. So, the average value is adopted in the analysis. A convenient figure of 415 kgs/cm^2 is adopted for the calculations.

CHAPTER III

ELASTIC ANALYSIS

It is endeavoured to correlate the experimental results with theoretical results in the elastic range. Approximate analyses are presented in the succeeding sections.

3.1 Introduction

There are Exact Theories to analyze the cylindrical shell, but these theories involve considerable amount of time. On the other hand, approximate theories involve a certain amount of error, but they are easy to be dealt with long shells. The Schorer Theory is simple and gives results with good accuracy in the case of long shells.

In the case of span/radius ratio ≥ 5 for shells without edge beams, it had been experimentally found that the distribution of stresses varies linearly. The ratio tends to reduce up to 3 for the shells with edge beams. Schorer himself has proposed the number of π , beyond which the shell can be treated as Long Shell. In accordance with A.S.C.E. classification for shells, the shell which exceeds the span/radius ratio of 3, is considered to be long shell.

The above propositions fulfil the requirements to make the shell under consideration as long shell.

As the Schorer Theory is simple, it is used to analyze the cylindrical shell.

The second approach attempted is simple Beam Theory. Beam Method is applicable for Long Shells. So, the method suits the present analysis.

Beam Method consists of two parts, one is Beam Analysis and another is Arch Analysis. Analysis by Beam Method is confined only to Beam Analysis in the present investigation. The shell in Beam Analysis is assumed to be a beam with curved cross-section.

3.2 General Solution

Initially, shell is considered to be in Membrane State. Membrane Solution can be found in the following way.

Membrane Solution

Three equilibrium equations in the membrane state, involve three unknown in-plane stress resultants. So, the solution of three equations derives three in-plane stress resultants. Membrane displacements are obtained from stress-strain relations.

Bending Solution

Membrane solution develops stresses at free edges. But physical boundary conditions do not allow the existence of such stresses. So, corrective line loads are introduced at the free edges to satisfy actual boundary conditions. These forces bend the shell, so bending solution is required to account for these effects. Bending solution is obtained by Schorer Theory.

General solution of the cylindrical shell is obtained by superimposing membrane solution over bending solution as the material is considered to be elastic.

3.3 Schorer Theory

3.3.1 Assumptions

The following assumptions in the Schorer Theory are taken

(a) The material is isotropic, homogeneous and elastic.

(b) The plane normal to the middle plane before bending remains plane normal to the middle surface.

(c) Stresses normal to the shell surface are neglected.

(d) All the displacements of the shell are small.

(e) Longitudinal Moment M_x, Transverse Shear in longitudinal direction Q_x and twist $M_{x\phi}$, are neglected.

(f) Tangential strain ϵ_ϕ and in-plane shear strain $\gamma_{x\phi}$ are neglected.

(g) Poisson's ratio is neglected.

The assumptions (a) to (d) are common to all bending theories and they stand for the problem. The forces mentioned in (e) are small compared to the transverse moment M_ϕ and the transverse shear Q_ϕ in long shells. Hence, they are neglected in the analysis. Likewise, the strains mentioned in (f) being small compared to longitudinal strain ϵ_x are neglected. Poisson's ration appears as the square of its own value in the expressions of stress resultants and displacements. So, the square of Poisson's ratio is very small compared to the unity. Hence, Poisson's ratio is neglected in the analysis.

3.3.2 Solution of the Cylindrical Shell as per Shorer

The assumptions yield a simple governing differential equation in terms of radial displacement as (6)

$$\frac{\partial^8 w}{\partial \phi^8} + \frac{12R^6}{t^2}\frac{\partial^4 w}{\partial x^4} = 0 \qquad (3.1)$$

Solution of w is sought in the following form

$$w = H e^{m\phi} \cos \frac{n\pi x}{L} \qquad (3.2)$$

where H - constant

The characteristic equation is obtained by substituting (3.2) in (3.1) and written as

$$m^8 + \frac{12n^4\pi^4R^6}{L^4t^2} = 0 \qquad (3.3)$$

The solution of (3.3) gives an infinite series for the expression of w. The first term of an infinite series is taken for the expression w and written as

$$w = [e^{-\alpha_1\phi}(A\cos\beta_1\phi + B\sin\beta_1\phi) + e^{-\alpha_2\phi}(C\cos\beta_2\phi + D\sin\beta_2\phi)]\cos\frac{\pi x}{L} \qquad (3.4)$$

where α_1, α_2 - Real Parts of Complex Roots

β_1, β_2 - Imaginary Parts of Complex Roots

A, B, C, D - Constants

The expressions for stress resultants and displacements can be written in terms of unknown

constants. Once the unknowns are evaluated from boundary conditions, then the stress resultants and displacements can be determined for any point on the shell.

3.4 Beam Theory

The assumptions (a) to (g) in Schorer Theory hold good for Beam Theory also.

Shell under consideration is taken as a flexural member. Hence, the membrane solution is absent in the Beam Theory.

Only the deflection is found by the beam analysis. The transverse deflection does not vary along the arc.

3.5 Boundary Conditions

The boundary conditions at two edges are the same because of the symmetry in geometry and loading. Hence, the boundary conditions at one edge are considered to be enough to solve the simultaneous equations. The boundary conditions at the junction of shell and edge beam are the following.

No Tie Bar Case

Edge beams are normally thin in the case of long shells. Consequently, their moment of inertia about vertical axis is negligible. So, edge beams are

not capable to withstand lateral thrust and transverse moment. So, two boundary conditions can be stated as

(i) The algebraic sum of the horizontal forces is zero

$$\sum H = 0.$$

(ii) The transverse moment is zero.

$$M_{\phi} = 0.$$

The compatibility of deformation at the junction of shell edge and edge beam gives two boundary conditions.

(iii) The longitudinal displacement u of the shell = That of the Edge Beam.

(iv) The vertical deflection of the shell = That of the Edge Beam.

Tie Bars Case

The introduction of the tie bars develops the resistance to the lateral thrust. Therefore, the first boundary condition in no tie bar case is altered. It is written as below

$$\sum H = f(x)$$

f(x) represents some resisting force developed due to the tie bar.

The remaining three boundary conditions in the former case are not altered.

Displacements would be changed in magnitude because of the tie bars, but the expressions for the longitudinal and the vertical displacements are unaltered, as the expressions for the stress-resultants and the displacements are functions of surface forces, not the boundary forces.

To avoid the mathematical complexities with the formulations of stress-resultants and displacements, the tie bar force is expressed as a Fourier series.

f(x) is expressed in the following form.

$$f(x) = \sum_{n=0}^{\infty} H_n \cos \frac{n\pi x}{L}$$

Origin of x is taken at the centre of the edge beam. The method to find H_n is illustrated in Appendix B.

3.6 Loading on the Shell

Two point loads, each at one-third of the span, were applied on the shell. It is desirable to keep the form of the loading consistent with the formulations of the stress resultants and the displacements. So, the loading taken in the analysis was expressed as

Fourier Loading. The method to find the Fourier Loading is briefly mentioned below.

The uniform load in longitudinal direction is found out by the virtual work concept. The deflection function in the virtual work concept is assumed as Sine function. Work done by the two point loads is equated to that by some assumed quantity of the uniform load. The equality computes the uniform load on the shell. This uniform load obtained is a line load acting at the ridge. The uniform load acting over the whole area is obtained from the line load by simple statics.

Finally, the uniform load in longitudinal direction is converted into Fourier Loading and the first term of the infinite series is considered for the loading. The whole method is illustrated in Appendix C.

3.7 Programme on the Computer

3.7.1 Introduction to the Programme

The analysis of the cylindrical shell is made by the Schorer Theory being programmed on the digital computer: IBM 7044-1401 systems. To make the expressions of the stress-resultants and the displacements in the matrix form, they are written in the following general form (6).

$$H_i = M_i \left[e^{-\alpha_1 \phi} \left\{ B1_i (A\cos\beta_1\phi + B\sin\beta_1\phi) + B2_i (B\cos\beta_1\phi - A\sin\beta_1\phi) \right\} + e^{-\alpha_2 \phi} \left\{ B3_i (C\cos\beta_2\phi + D\sin\beta_2\phi) + B4_i (D\cos\beta_2\phi - C\sin\beta_2\phi) \right\} \right] \quad -(3\text{-}5)$$

for i = 1, 8

H_i Any Shell Action

i=1,8 It may be the stress resultant or the displacement.

M_i - Corresponding Multiplier which is constant term

i=1,8

$(B1, B2, B3, B4)_i$ - Corresponding coefficients expressed

i=1,8 in terms of the roots

$\alpha_1, \alpha_2, \beta_1, \beta_2$ - Roots of the characteristic equation.

A, B, C, D - Arbitrary constants

H_i is illustrated as below

$$H_{i\ i=1,8} = \left[N_{x\phi},\ Q_\phi,\ N_\phi,\ M_\phi,\ u,\ w,\ v,\ \vartheta \right]$$

The values of $M_{i\ i=1,8}$ and $(B1, B2, B3, B4)_{i\ i=1,8}$ are shown in the Tables D-1 and D-2 given in Appendix D.

As the number of the unknown constants is 4, the number of the shell actions is taken as 4 for the matrix computations. So, H_i $\underset{i=1,8}{}$ is equally divided into two parts. One part is for the stress resultants and another part is for the displacements. So, the dimension of the matrix [H] becomes 4 x 1.

For the matrix computations, the right-hand side of the equation (3.5) is cast in the following form.

$$[H]_{4x1} = [M]_{4x4}\,[B]_{4x4}\,[F]_{4x4}\,[X]_{4x1} \tag{3.6}$$

$$= |Z|_{4x4}\,|X|_{4x1} \tag{3.7}$$

where $[Z] = [M][B][F]$

Matrices in (3.6) are briefly explained.

Matrix [H] consists of the stress-resultants or the displacements. Matrix [M] stands for the multipliers of the stress resultants or the displacements. Matrices $[M]^s$ can be generated from Table D-1. Only the diagonal terms in the matrix [M] exist and off-diagonal terms are zero. Matrix [B] is a function of the roots of the characteristic equations. Matrices

$[B]^S$ for the stress-resultants and the displacements can be generated from the Table D-2.

Matrix F is indicated below

$$= \begin{bmatrix} e^{-\alpha_1\phi}\cos\beta_1\phi & e^{-\alpha_1\phi}\sin\beta_1\phi & 0 & 0 \\ -e^{-\alpha_1\phi}\sin\beta_1\phi & e^{-\alpha_1\phi}\cos\beta_1\phi & 0 & 0 \\ 0 & 0 & e^{-\alpha_2\phi}\cos\beta_2\phi & e^{-\alpha_2\phi}\sin\beta_2\phi \\ 0 & 0 & -e^{-\alpha_2\phi}\sin\beta_2\phi & e^{-\alpha_2\phi}\cos\beta_2\phi \end{bmatrix}$$

Matrix $[F]$ is not altered in the case of the stress resultants or the displacements. It depends on the roots and the angle.

Matrix $[X]$ is indicated below

$$= \begin{bmatrix} A \\ B \\ C \\ D \end{bmatrix}$$

Matrix $[X]$ is a function of only arbitrary constants, so it is not influenced by the stress resultants or the displacements.

For the sake of convenience in the computations, [H] is separately designated as [HF] and [HD] for the forces and the displacements respectively. F and D letters denote the forces and the displacements respectively. Similarly [MF], [MD], [BF], [BD], [ZF], [ZD] follow the same notation. [F] matrix remains the same for [HF] or [HD] as explained earlier. [X] matrix is also unaltered. Matrix [X] is to be obtained from a set of boundary conditions.

Once, the arbitrary constants are evaluated, then they are substituted in (3.5) to compute the shell actions. The resultant shell action at any angle from the edge is derived by superimposing the effects originating at an angle of $(2\phi_c - \phi)$ over the corresponding terms at an angle of ϕ. For symmetric functions involving even derivatives of ϕ, these two effects are to be added. But for antisymmetric functions which involve odd derivatives of ϕ, these two effects are to be deducted. These resultant shell actions are for bending solution. Final solution for the shell actions is obtained by superimposing membrane solution over bending solution.

3.7.2 Operations

As explained in 3.2, membrane forces and displacements were computed. Roots of the characteristic equation were found for the bending solution. Matrices

$[MF]$, $[MD]$, $[BF]$, $[BD]$ were generated and stored in the memory location. Respective matrices $[M]$ and $[B]$ for the forces and the displacements were multiplied. Matrix $[F]$ at an angle ϕ was developed and subsequently it was multiplied with the product of $[M][B]$. Matrix $|F|$ at angle of $(2*\phi_c - \phi)$ was generated and similar operation was carried. Rows of $[M][B][F]_{near}$ and $[M][B][F]_{far}$ were added or subtracted depending on the properties of the shell action. Final matrices for the forces and the displacements were designated as $[ZF]$ and $[ZD]$ respectively.

Next step was to evaluate matrix $[X]$ from the boundary conditions. Governing equation for evaluating constants is written as

$$[C][X] = [Y] \tag{3.8}$$

$[C]$ matrix was derived from a set of four boundary conditions. $[C]$ is depending on the bending solution, but is not influenced by the change in the boundary conditions under consideration. Matrix $[Y]$ takes care of the change in the boundary conditions. $[Y]$ depends on the Membrane Solution also.

A brief explanation for matrix $[Y]$ is required before Equ. (3.6) is executed for the boundary conditions for the tie bars.

In the case of B.C. for no tie bar, Equ. (3.6) has multiplier $\cos \frac{\pi x}{L}$ on both sides. So, the multiplier gets eliminated during the execution of (3.6). But in the case of B.C. for the tie bars, the first element of $[Y]_{4x1}$ involves the constant term. The constant term appears because the tie bar force is expressed into Fourier Series. This can be seen from Appendix B. To avoid this mathematical complexity, first rows of $[C]$ and $[Y]$ were orthogonalized. Consequently, first rows of $[C]$ and $[Y]$ did not contain any circular function. Orthogonalization facilitated the matrix computations. Orthogonalization of the functions is shown in Appendix B.

From equation (3.8)

$$[X] = [C]^{-1} [Y] \qquad (3.9)$$

Inversion of matrix $[C]$ was done by Gauss-Seidel Method. (3.9) expression gives solution for arbitrary constants.

No Tie Bar Case

Case of no-tie bar is very simple for the determination of shell actions. Arbitrary constants A, B, C, D were substituted in (3.5). Superposition concept for the bending and the membrane solution was applied to compute the forces and the displacements at the points under consideration.

Tie Bars Case

Three stages of shell are considered to incorporate the tie bar effect.

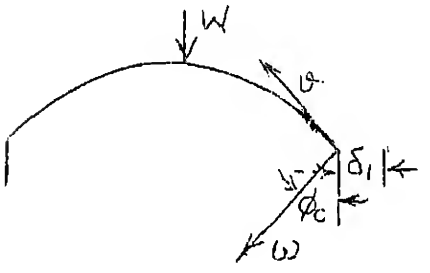

(Point load is considered only to illustrate the method)

Fig. 3.1 Shell with Load

In the first instance, the horizontal displacement δ_1 at the tie bar location, but without considering the presence of the tie bar, is found by using the following expression

$$\delta = v \cos \phi_c + w \sin \phi_c \qquad (3.8)$$

ϕ_c = Semi - Central Angle

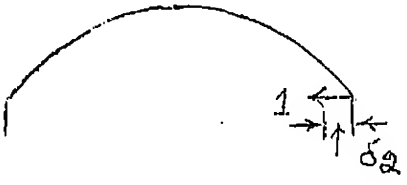

Fig. 3.2 Shell with Unit Tie Force

In the second instance, unit tie force is applied to resist outward displacement. And, δ_2 displacement is found.

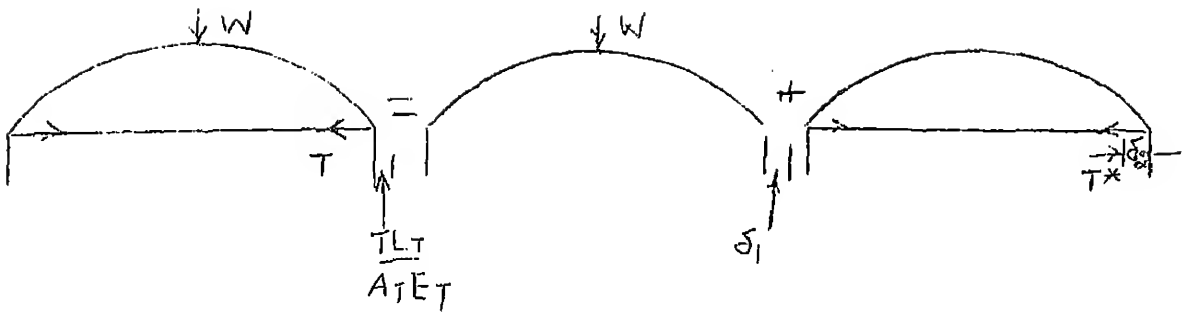

Fig. 3.3 Illustration of Superposition Principle

In the third step, effects due to W and T are superimposed over each other. The following equation from Fig. 3.3 and can be written

$$\delta_1 + T\delta_2 = \frac{TL_T}{A_T E_T} \qquad (3.9)$$

$$T = \frac{\delta_1 A_T E_T}{L_T - \delta_2 A_T E_T} \qquad (3.10)$$

This value of T was substituted in (B-8) to (B-12) for different cases. Thus, first element of [illegible] was formed for all the cases.

As explained in no tie bar case, forces and displacements at points under consideration were found for all load increments.

3.7.3 Flow Chart

Flow Chart is drawn to explain the procedure described in 3.7.1 and 3.7.2.

FLOW--CHART

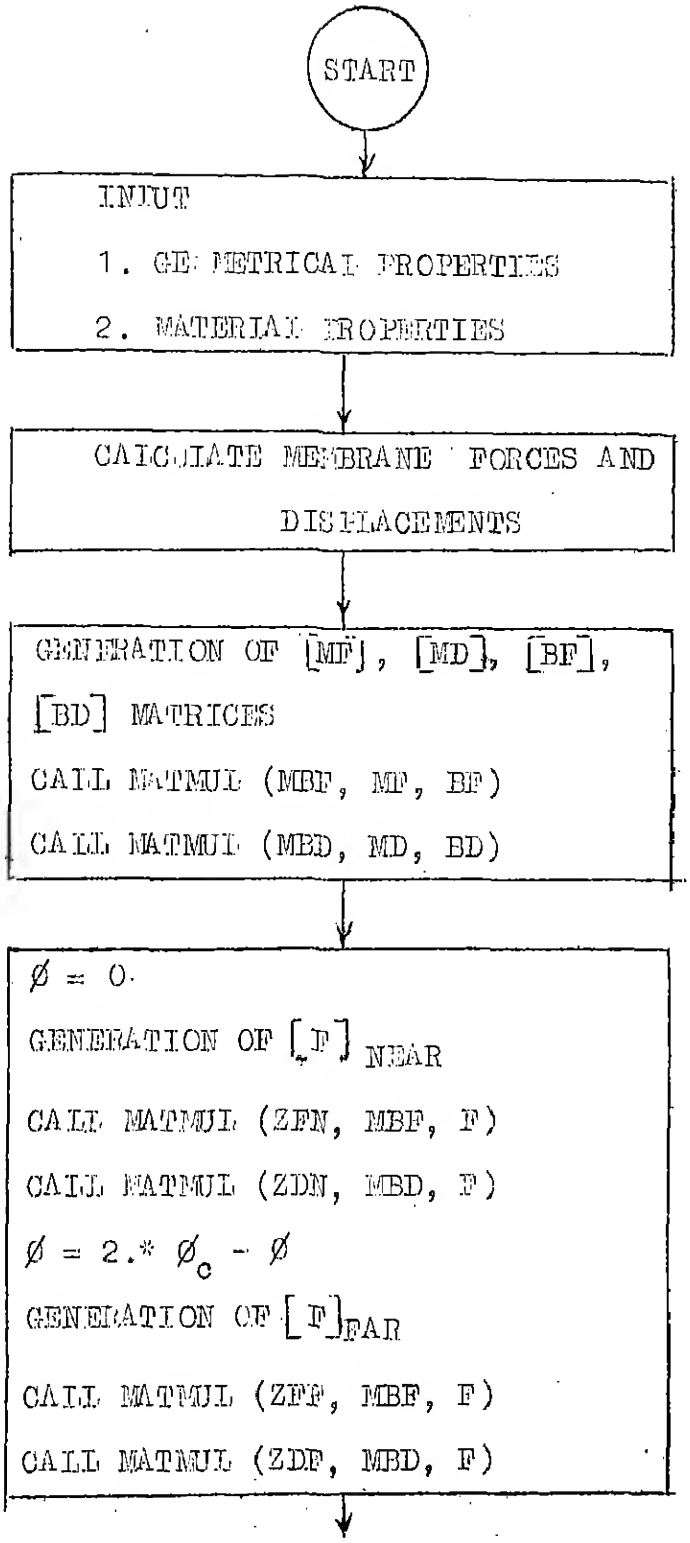
START
INPUT
1. GEOMETRICAL PROPERTIES
2. MATERIAL PROPERTIES
CALCULATE MEMBRANE FORCES AND DISPLACEMENTS
GENERATION OF [MF], [MD], [BF], [BD] MATRICES
CALL MATMUL (MBF, MF, BF)
CALL MATMUL (MBD, MD, BD)
∅ = 0.
GENERATION OF [F]NEAR
CALL MATMUL (ZFN, MBF, F)
CALL MATMUL (ZDN, MBD, F)
∅ = 2.* ∅c - ∅
GENERATION OF [F]FAR
CALL MATMUL (ZFF, MBF, F)
CALL MATMUL (ZDF, MBD, F)

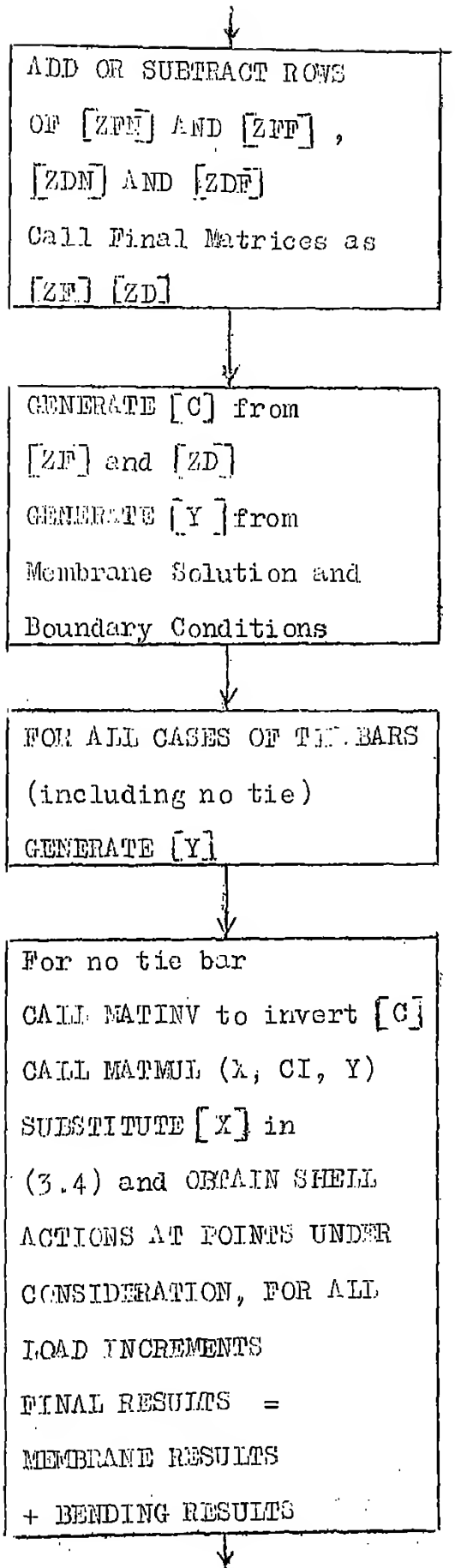
ADD OR SUBTRACT ROWS
OF [ZFN] AND [ZFF] ,
[ZDN] AND [ZDF]
Call Final Matrices as
[ZF] [ZD]
GENERATE [C] from
[ZF] and [ZD]
GENERATE [Y] from
Membrane Solution and
Boundary Conditions
FOR ALL CASES OF TIE BARS
(including no tie)
GENERATE [Y]
For no tie bar
CALL MATINV to invert [C]
CALL MATMUL (X, CI, Y)
SUBSTITUTE [X] in
(3.4) and OBTAIN SHELL
ACTIONS AT POINTS UNDER
CONSIDERATION, FOR ALL
LOAD INCREMENTS
FINAL RESULTS =
MEMBRANE RESULTS
+ BENDING RESULTS

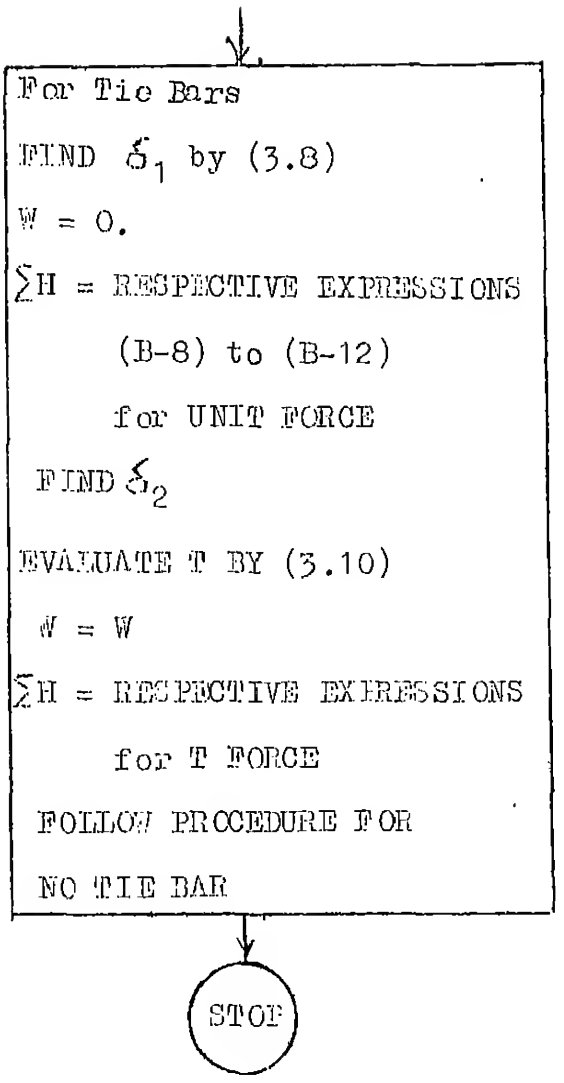
For Tie Bars
FIND δ_1 by (3.8)
W = 0.
$\sum$H = RESPECTIVE EXPRESSIONS
(B-8) to (B-12)
for UNIT FORCE
FIND δ_2
EVALUATE T BY (3.10)
W = W
$\sum$H = RESPECTIVE EXPRESSIONS
for T FORCE
FOLLOW PROCEDURE FOR
NO TIE BAR
STOP

CHAPTER IV

RESULTS AND DISCUSSION

4.1 Deflection

Experimental Results

The deflections as mentioned in Section 2.4, were measured at the points shown in Fig. 2.6. Deflection curves are plotted in Fig. 4.1 for different number of the tie bars. It was observed that the deflection of the shell with one tie bar at the centre is less than that of the shell with no tie bar. Similar trend is seen for the shell with two tie bars. The percentages of reduction in experimental deflections were approximately 10% and 15% respectively.

The deflection of the shell with three tie bars is more than that of shell with two tie bars. This may not seem true. In the case of CS3, two bars other than central bar were placed near support. So, naturally, these two bars did not give significant contribution in reducing deflection. So, this indicates that not only number of tie bars, but also their position matters.

It is observed from Fig. 4.1 that as the number of the tie bars is increased, the corresponding deflection is not proportionately decreased. The load deflection

curves are shown in Fig. 4.2 for the centre point. All the shells showed a consistent behaviour.

It was thought to find some parameter which might govern the spacing of the tie bars. Some relation can be established between the ratio chord width to the spacing and the deflection. As the spacing decreased, the deflection decreased.

Centre deflections for various chord width/ spacing ratios are shown in Table 4.1. The percentages of reductions in deflections are mentioned with respect to the centre deflection of the shell with no tie bar. The results are also plotted in Fig. 4.3. It is observed from the Fig. 4.3 that when the chord width/spacing ratio is nearly unity, the corresponding layout of the tie bars yields optimum results. And onwards, the curve behaves asymptotically.

Chord Width/Spacing of tie bars	Deflection Cro	Reduction Percentage in deflection w.r.t. that of CS0
0.347 - CS0	0.0805	0.0
0.725 - CS1	0.0735	8.7
1.050 - CS2	0.0680	14.3
2.075 - CS5	0.0660	18.0

Table 4.1 - Deflections Against Chord Width/ Spacing Ratios

Theoretical Results by Schorer Theory

The deflections in the shell with no tie bar are plotted in Fig. 4.4. The deflections obtained from the Schorer Theory using the equivalent distributed load based on virtual work concept are 25% less as compared to the experimental results. The present experimental deflections are caused due to two point loads. While, the loading in the analysis is considered as uniform loading. Hence, this leads to greater experimental results compared to the theoretical results under consideration.

The theoretical results could not be derived for the shells with the tie bars. This happened because of the different form of the loading considered in the analysis. The shell had flattened out due to the point loads. And, this flattening was partially restrained by the tie bars. But the uniform loading considered made the shell edges to move inward. The prediction of the vertical deflections using an equivalent distributed load based on virtual work concept is fairly close whereas the lateral displacements between the theory and the experiments do not agree at all.

The tie bars would do their function when the shell flattens out. The flattening can occur in the following instance.

When the edge beams are very stiff, then the equation (3.9) can be applied. The shell with the stiff edge beams would flatten even if the loading on the shell is uniform.

The horizontal edge displacement may be expressed as

$$\delta_h = \delta_{hm} + \delta_{hb} \qquad (4.1)$$

where,

δ_h = Net Horizontal Displacement

δ_{hm} = Membrane Horizontal Displacement

δ_{hb} = Bending Horizontal Displacement

Fig. 4.5 – Displacements in Shell

$$\delta_h = w \sin \phi_c + v \cos \phi_c$$

δ_h is positive when it is inward.

$$\delta_{hm} = w_m \sin \phi_c + v_m \cos \phi_c$$

$$= \frac{8w_u}{Emt}\left[2\left(\frac{L}{\pi}\right)^2 + \frac{1}{R^2}\left(\frac{L}{\pi}\right)^4\right]*$$

$$\left[\sin \phi_c \cos \phi_c - \sin \phi_c \cos \phi_c\right] \cos \frac{\pi x}{L}(s)$$

$$= 0.$$

So, the membrane horizontal displacement is zero. The point moves downward, but does not move horizontally. So, only the bending displacement decides about the introduction of the tie bars.

The solution of the shell with the edge beams can be found by superimposing the effect of the edge beams over the solution of the shell with free edges. The membrane solution gives the forces at the free edges. The edges are made free by applying the corrective forces or line loads V_L, H_L and S_J shown in Fig. 4.5. The corrective forces are opposite to the membrane forces at the edge. The directions of the forces shown in Fig. 4.6 are positive.

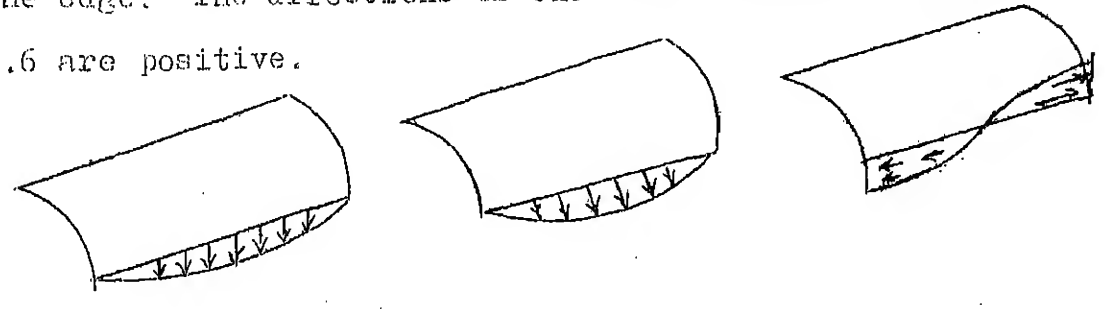

Vertical Force V_L Horizontal Force H_L Shear Force S_L

Fig. 4.6 - Corrective forces at Free Edge

The effect of the edge beam is added to arrive at the final solution. As the beam is normally slender, it does not offer resistance to rotation and horizontal translation. So, only the two forces, vertical force V_b and shear force S_b are considered.

V_b generally acts upward on the shell and downward on the beam. S_b generally acts inwards on the shell and outward on the beam. These forces on the shell are opposite to the corresponding line forces. The forces are shown in Fig. 4.7.

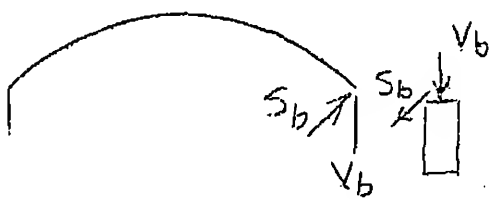

Fig. 4.7 - Beam Forces

V_b and S_b forces are to be found from compatibility equations of the displacement and stress at the junction of shell edge and edge beam.

Bending horizontal translation of the shell edge is caused due to the forces shown in Fig. 4.5 and 4.6. The expression is written as (5)

δ'_s are the coefficients for the respective line loads. And, they can be taken from the Table 2B, ASCE Manual: 31 "Design of Cylindrical Concrete Shell Roofs". First suffix indicates the horizontal displacement and the second suffix denotes the respective force which causes the displacement.

The term δ_{hh} contains negative sign, because the positive corrective force H_L produces negative horizontal displacement. Similarly, the displacements caused by V_b and S_b are negative.

Equ (4.2) can be reorganized and written as

$$\delta_h = \frac{L^4}{R^3 tE}\left[\delta_{hv}\,(V_L - V_b) - \delta_{hh}\,H_L - \delta_{hs}\,(S_b - S_L)\right] \qquad (4.3)$$

The condition for the provision of the tie bars is that the expression (4.3) should be negative indicating outward horizontal deflection. S_b is usually larger than S_L. So, the second and third terms yield outward translation. To make the expression negative,

$$\delta_{hv}\,(V_L - V_b) < \delta_{hh}\,H_L + \delta_{hs}\,(S_b - S_L) \qquad (4.4)$$

This implies that V_b should possess high value

or nearly equal to V_I. In other words, the edge beams should be so stiff that sufficient vertical resistance satisfying (4.4) should be offered by the edge beams.

The shell without edge beams would not get the vertical resistance at the edge, so the shells with uniform loading would hardly require the tie bars.

Once, the need to provide the tie bars in the shell exists, the shell with the tie bars can be analyzed by the method described in 3.7.2.

Theoretical Results by Beam Method

The deflections obtained from the Beam Theory are shown in Fig. 4.4. The theoretical deflections are less compared to the experimental results. The discrepancy is explained in the discussion for the Theoretical Results by the Schorer Theory. The deflections by the Beam Theory are higher than those by the Schorer Theory.

Comparative study among the results derived from various approaches is made in Fig. 4.3. It is found that the theoretical vertical deflections do not deviate much from the experimental results.

4.3
4.2 Tie Bar Force

Load V, ... Tie Bar Force graphs are shown in Fig. 4.8 and 4.9. Fig. 4.8 gives a study of the force developed in the central tie bar when CS1, CS3, CS5 are loaded. Similarly, Fig. 4.9 gives a study of the force developed in the tie bar placed at L/6 from the centre when CS2, CS4, CS5 are loaded.

The force in the central tie bar of CS1 is about twice of that of CS5. The difference between the central tie bar forces developed in CS1 and CS3 is not significant. This proves that the tie bars provided near the support do not yield remarkable contribution. There is considerable difference between the forces in the tie bars at L/6 from the centre, being provided in CS2 and CS4. But, the tie bar forces developed in CS4 and CS5 are approximately equal. So, it can be concluded that as the number of the tie bars increases beyond certain limit, the particular tie bar force behaves asymptotically.

The results of Load V, Total Tie Bar force along the span are plotted in Fig. 4.10. As the number of the tie bars increases, the total tie bar force increases. It is observed that the total tie bar force in CS3 is less than that in CS2. This can mathematically

be proved also. Equns. B-9 for CS2 and B-10 for CS3 derive the values of $\frac{4T}{L} * 3.087$ and $\frac{4T}{L} * 2.7815$ respectively. So, this proves that the total tie bar force in CS2 is greater than that in CS3.

Fig. 4.11 shows the variation of the tie bar force along the span. Experimental variation of the tie bar force is in Cosine form which is consistent with that adopted in the analysis.

4.3 Ultimate Strength

Load-deflection curves indicating inelastic behaviour are shown in Fig. 4.13. The deflections were measured up to certain loads and not up to failure. The measured deflections to the corresponding applied loads are shown in Fig. 4.13 It is observed that as the number of the bars increases, corresponding ultimate strength increases. Shell with no tie bar failed at 4100 kgs. Shell with one tie bar at the centre failed at 5000 kgs. This implies that the introduction of the tie bar increases ultimate strength but not largely. Shells with three tie bars and five tie bars failed at 6000 kgs and 6600 kgs respectively.

Fig. 4.12 gives an idea how the ratio of the chord width to the tie spacing affects the ultimate strength. Ultimate strength increases rapidly up to the chord width to spacing ratio being 2. Then, it does not increase significantly and the curve behaves asymptotically.

4.4 Comparative Study of Cylindrical Shell and Folded Plate

One of the objectives is to compare the stiffness of the identical cylindrical shell with that of the folded plate (7). The span, width, and rise are the same in both the specimens. The reinforcements in the two specimens are not equal. It is intended to know the qualitative picture for the comparison of the two structures. The results of the folded plate (7) are herein reproduced. Fig. 4.14 gives the comparative study of the cylindrical shell and the folded plate with no tie bar and the tie bars.

The deflection in the shell with no tie bar is about one-fourth of that in the folded plate with no tie bar in the elastic range. The deflection in CSO is about one-tenth of that in FPO in inelastic behaviour. So, the cylindrical shell is very stiff compared to the folded plate. So, a thinner section of the shell can be adopted to do the same work done by the folded plate.

The deflection in CS1 is about one-third of that in FP1 in the elastic range. The introduction of the tie bar in the cylindrical shell reduces the deflection by about 10%, while the tie bar in the folded plate reduces the deflection by about 40% in the elastic range. The deflection in CS1 is very much less

compared to that in FP1 in inelastic range.

There is no sharp increase in the deflection after the crack appears in the cylindrical shell. While, the deflection in the folded plate increases suddenly as soon as the crack develops.

4.5 Cracking Pattern and Mode of Failure

Shell with No Tie Bar

First cracks had developed at the junction of the shell edge and the edge beam due to bending. Cracks occurred in the transverse plane of loading. This plane was subjected to maximum moment and shear simultaneously, and hence, cracks were produced along this section. Cracks were not completely open through edge beam. Cracks had originated from the point where curvature of shell changed suddenly. And, this change created stress concentration in the area of junction.

It was found that there was no drop in load when first crack developed.

Flexural crack developed at the centre of edge beam with further increase in the load. As more load was applied, shear cracks developed in the corners of shell. Bending cracks did not propagate considerably, which showed the shell might not fail in bending.

Shear cracks progressed inwards rapidly, before ultimate load was reached. At ultimate load, shear cracks widened and penetrated deep into the edge beam. Shear cracks were joined on the underside of shell. This mechanism of failure is seen in Photograph 5.

Fig. 4.15 (a) to (d) gives the crack pattern. The crack pattern is shown in Photographs 4 and 5.

Effect of the Tie Bars on the Crack Pattern

Introduction of the tie bars did not affect the cracking load largely and mode of failure. But, as the load increased, the number of the flexural cracks and shear cracks increased. Flexural cracks were uniformly distributed, and these cracks were not very remarkable. And, cracks were not propagating at the rate which was in CS0. This distribution of cracks and their propagation might have contributed towards an increase in ultimate strength of shells with tie bars.

In the case of shell with five tie bars, longitudinal crack and diagonal cracks were joined at failure load. Longitudinal crack was developed due to yielding of transverse steel.

Crack patterns for CS1, CS3, CS5 are shown in Fig. 4.16, 4.17, 4.18 respectively.

Effect of the Tie Bars on the Crack Propagation

It was thought to study the effect of the tie bar on the existing crack in the shell. This study was taken with particular view. Normally, cracks develop at the junction of shell and edge beam. It becomes very difficult to prevent propagation of cracks. It was thought that introduction of tie bar at the point where crack had originated, might stop or reduce the rate of propagation. In this regards, experiment was carried in the same way as described in Chapter II.

Last specimen with no tie bar was taken before it was finally loaded up to failure. Specimen was slowly loaded until it got distinct crack. This crack had originated from the hole spaced at L/6 from the centre. Then, the load was removed from the shell. The tie bar was introduced at the crack location. The shell was again loaded. But, the crack did not open at previous cracking load. Shell was further loaded, but crack did not open. Afterwards, shell was unloaded and the same specimen with five tie bars was tested up to failure, but the original crack did not make a way to propagate.

The above phenomenon indicates that if crack in the existing structure is not wide, introduction of tie bar at the crack location reduces the propagation of the crack.

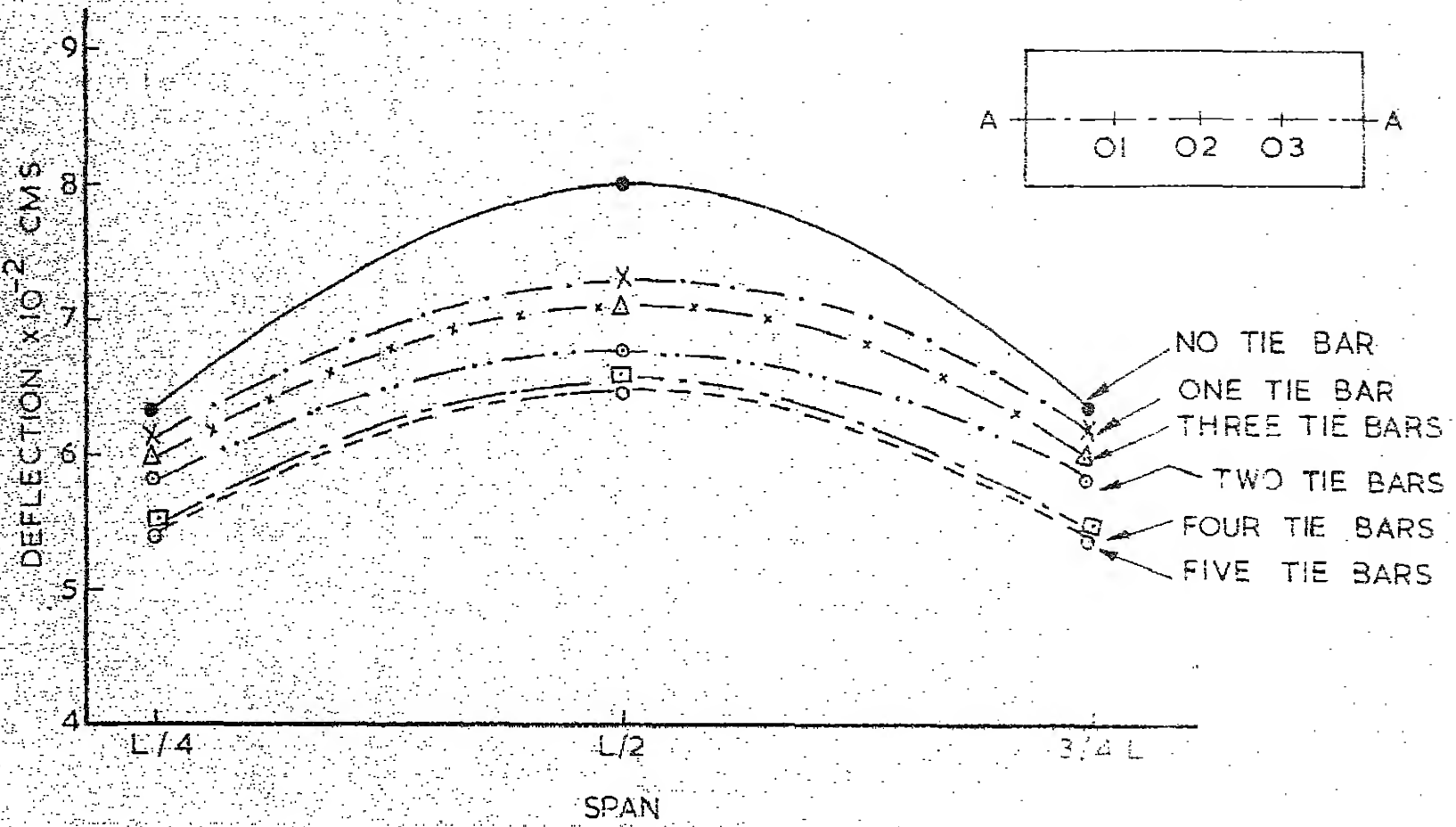

FIG. 4.1 EFFECT OF TIE BAR SPACING ON DEFLECTION ALONG THE SECTION A A (LOAD = 910 KGS)

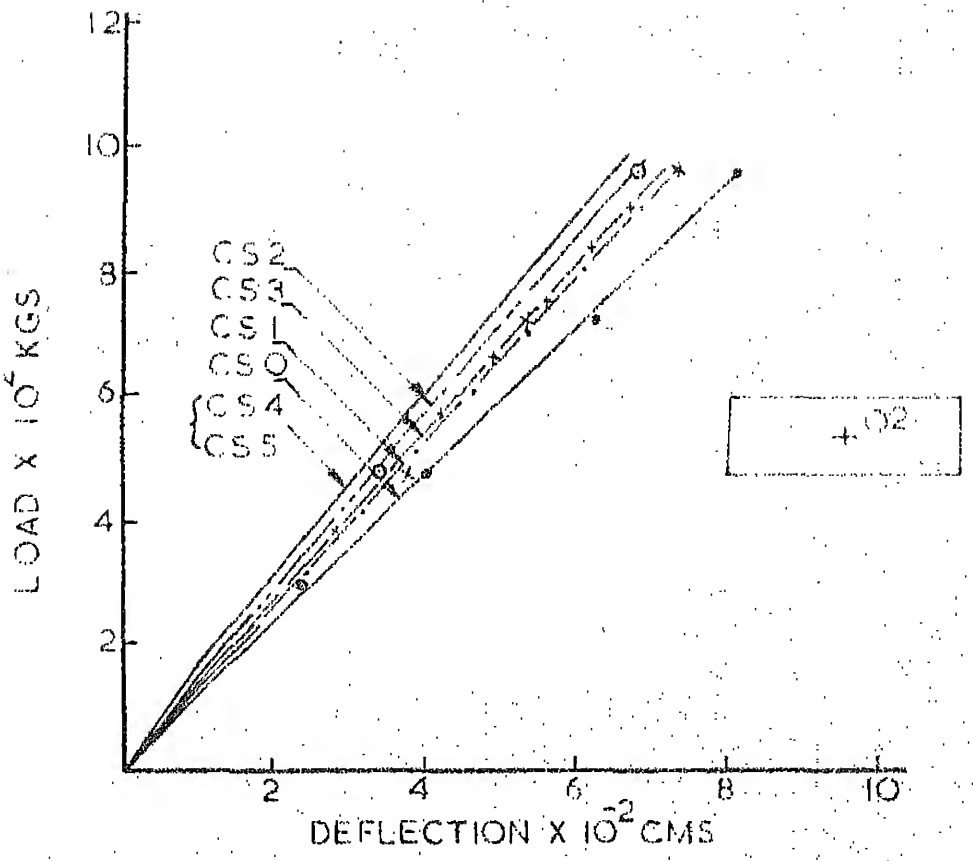

FIG. 4·2 EFFECT OF TIE BARS ON DEFLECTION AT A POINT : 0.2

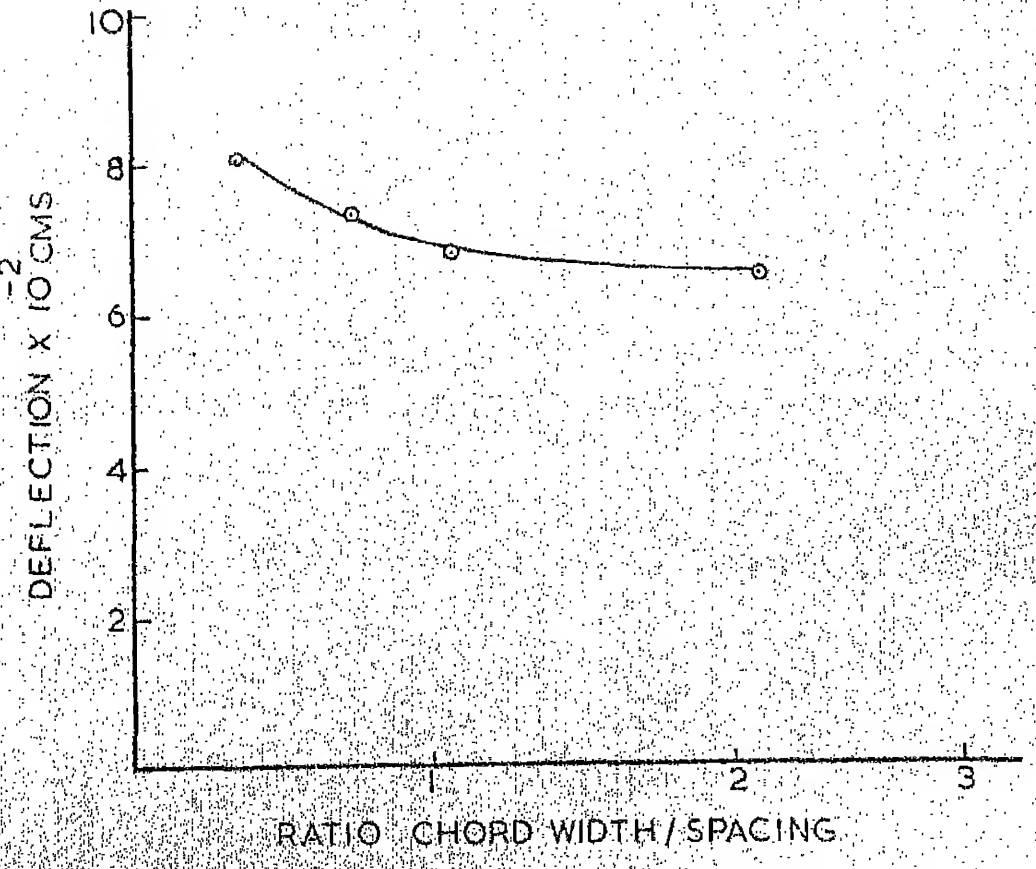

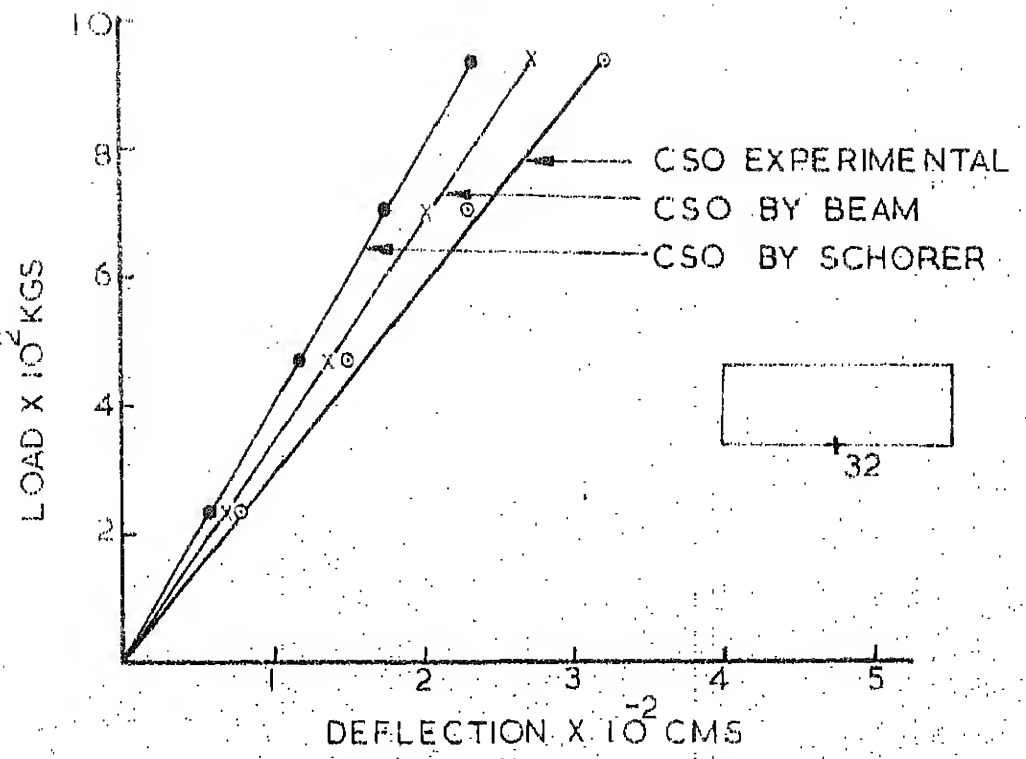

FIG. 4.4 COMPARATIVE STUDY OF DEFLECTION

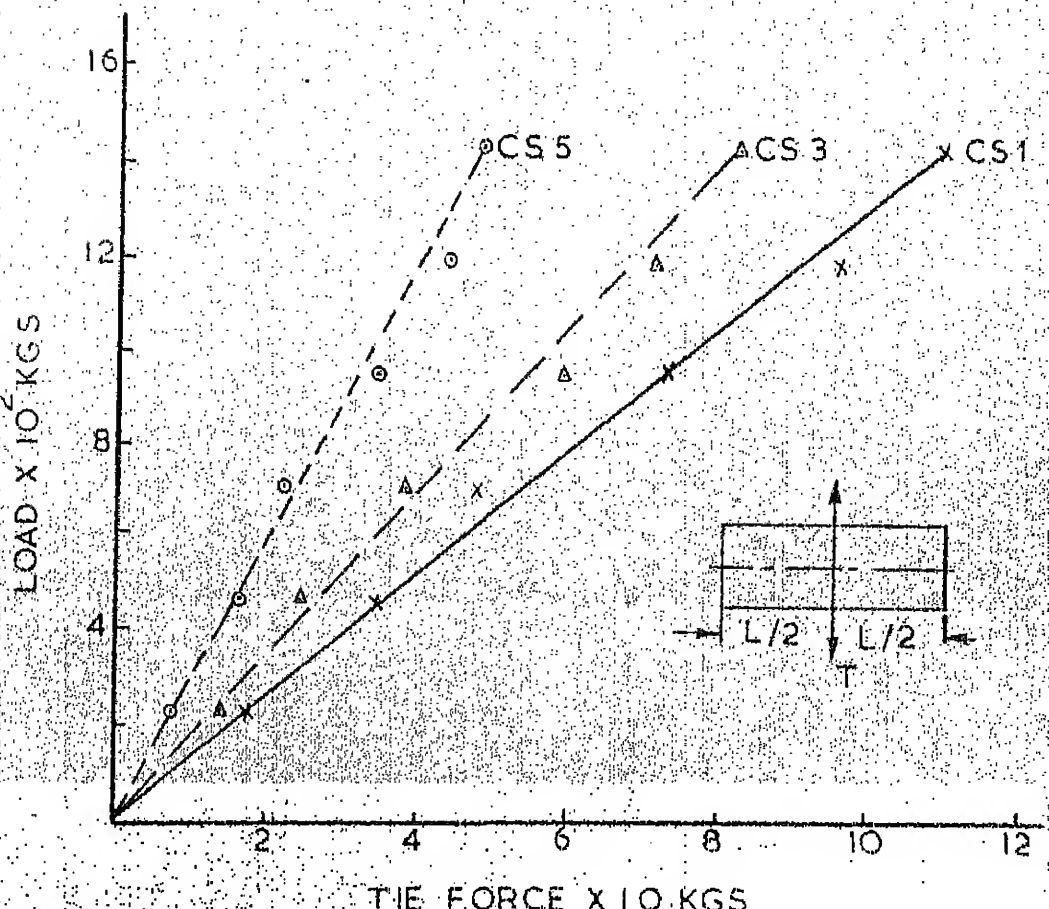

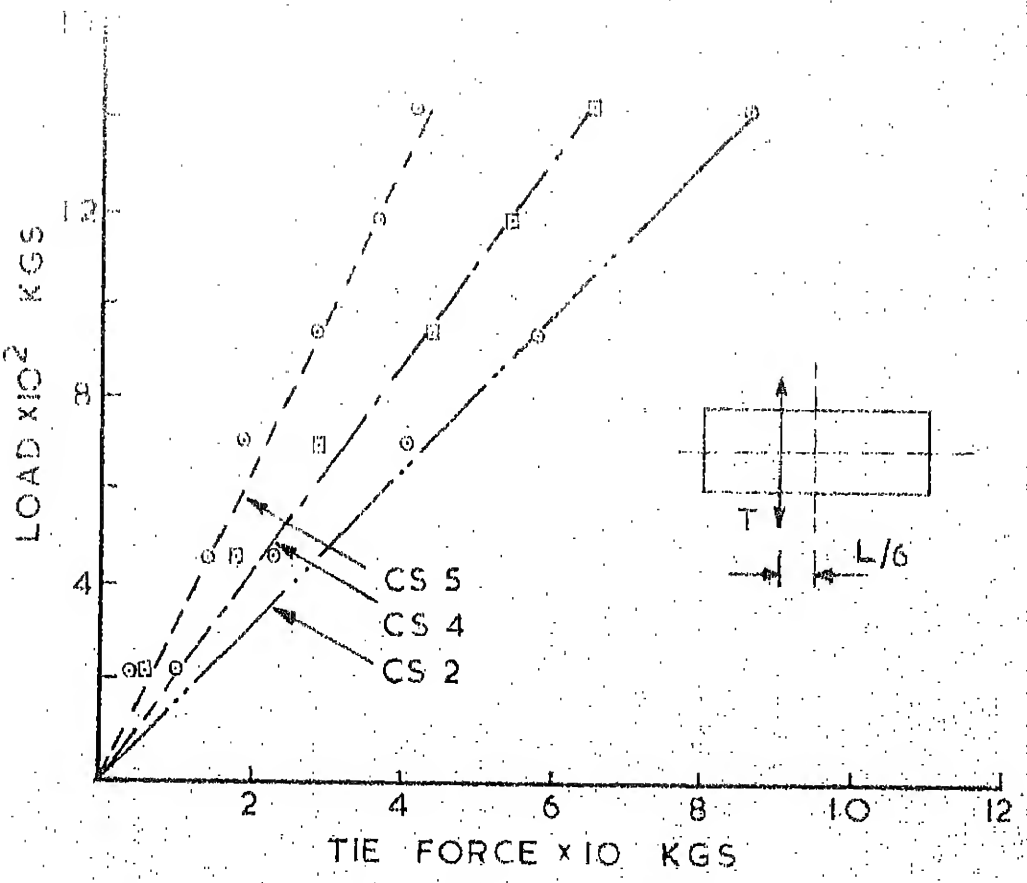

FIG. 4·9 LOAD VS TIE FORCE AT CERTAIN LOCATION.

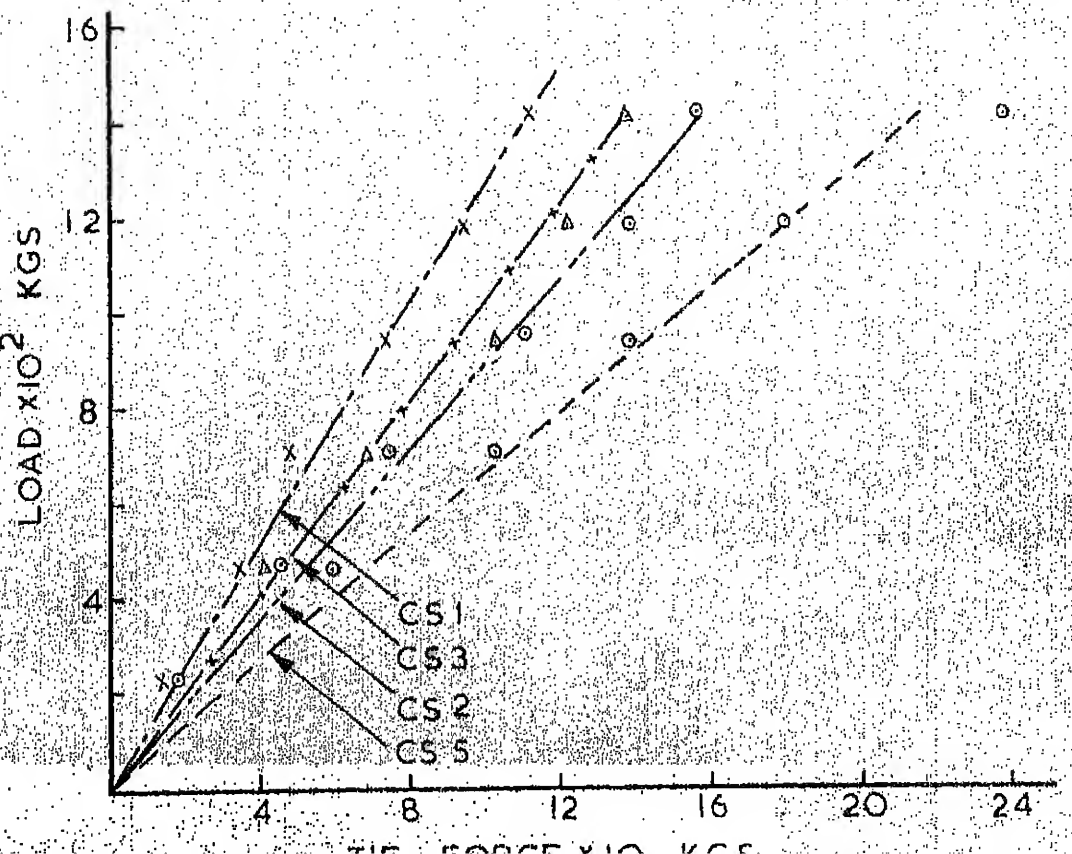

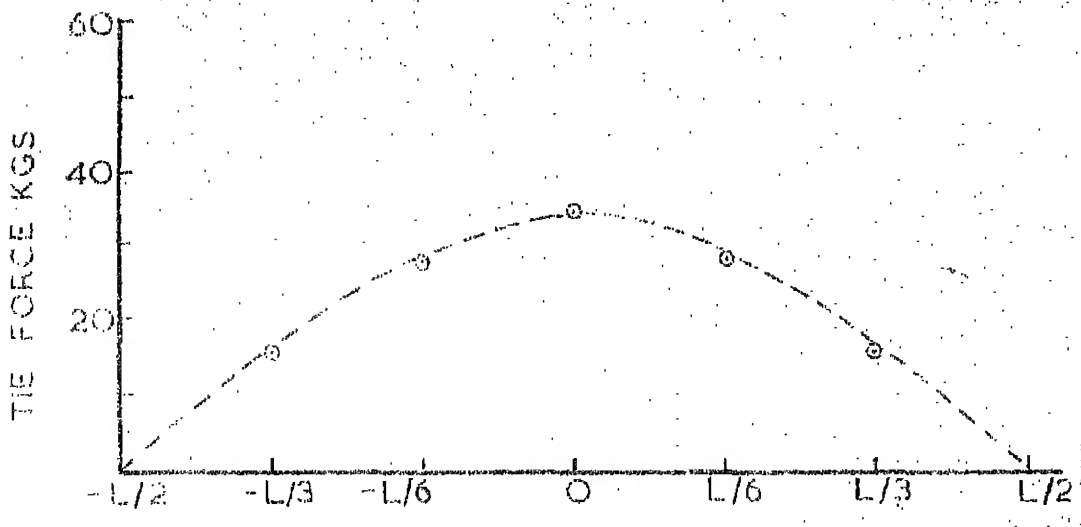

FIG-4-11 TIE FORCE VARIATION ALONG SPAN

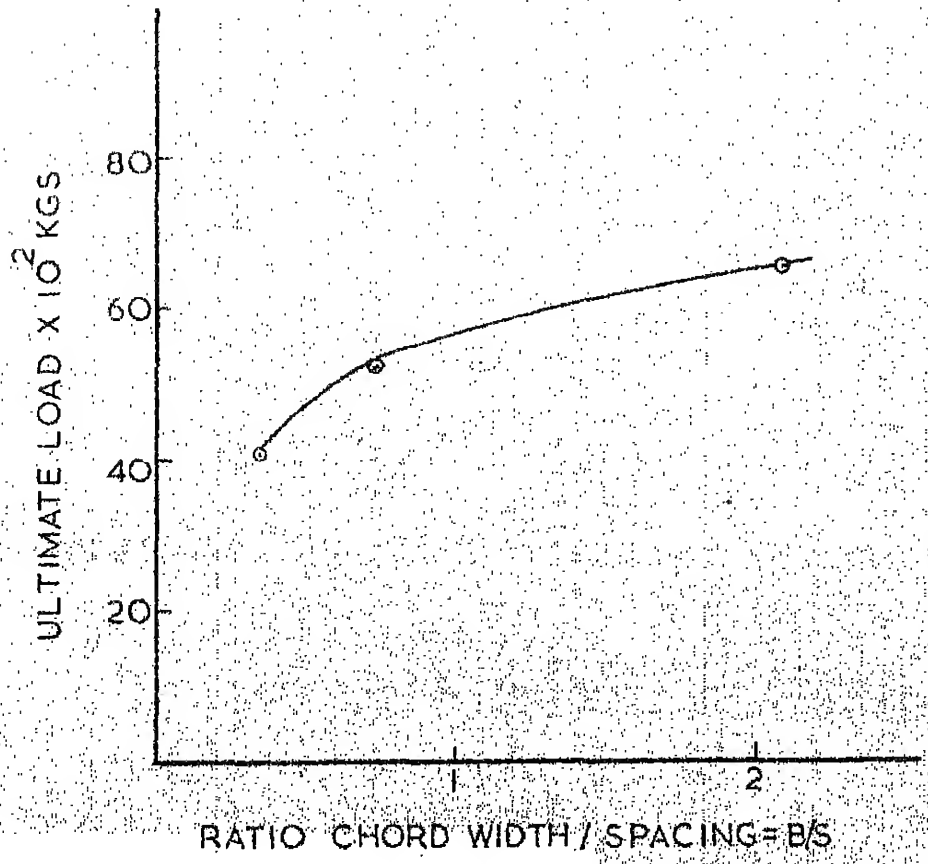

FIG-4-12 ULTIMATE STRENGTH VS RATIO B/S

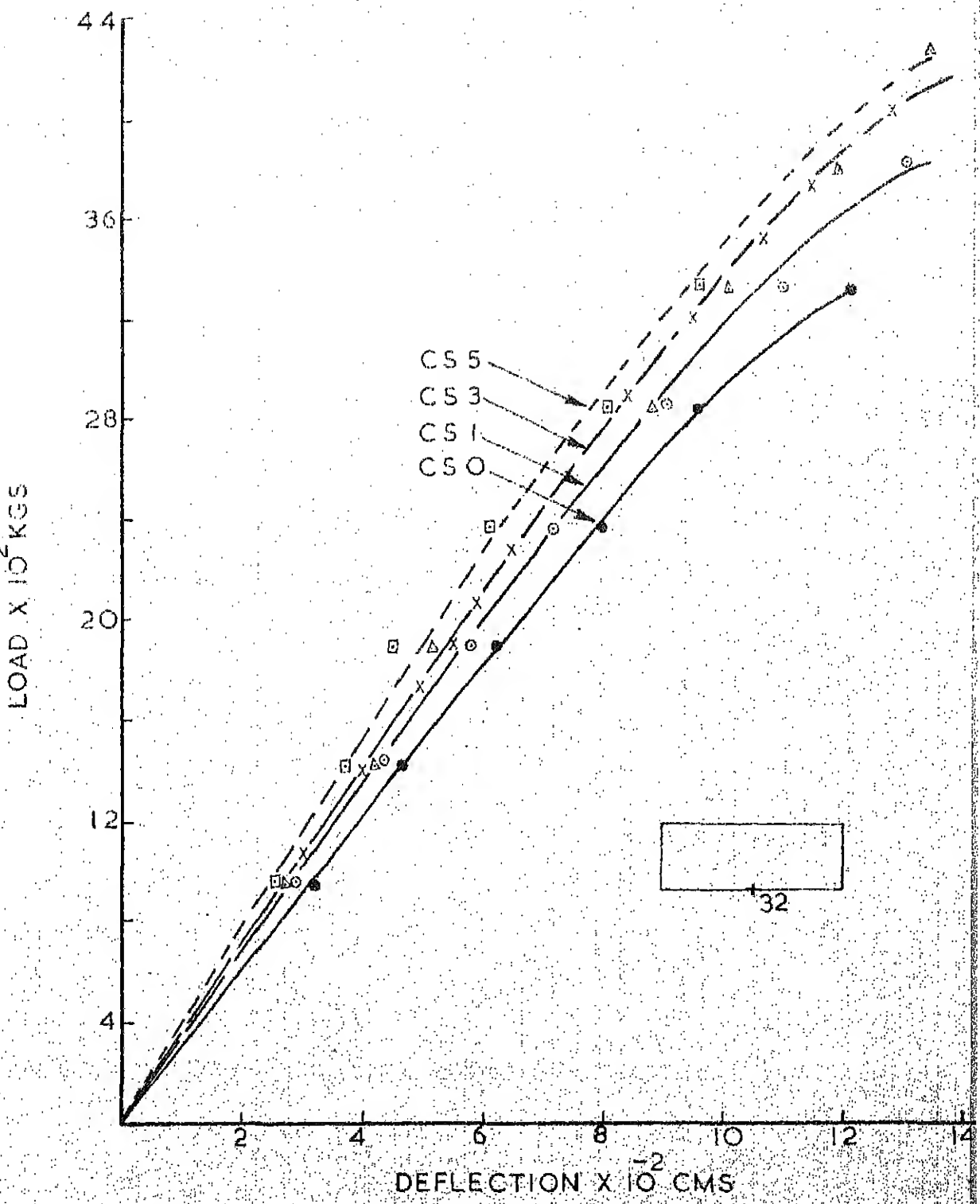

FIG. 4.13 EFFECT OF TIE BARS ON ULTIMATE BEHAVIOUR

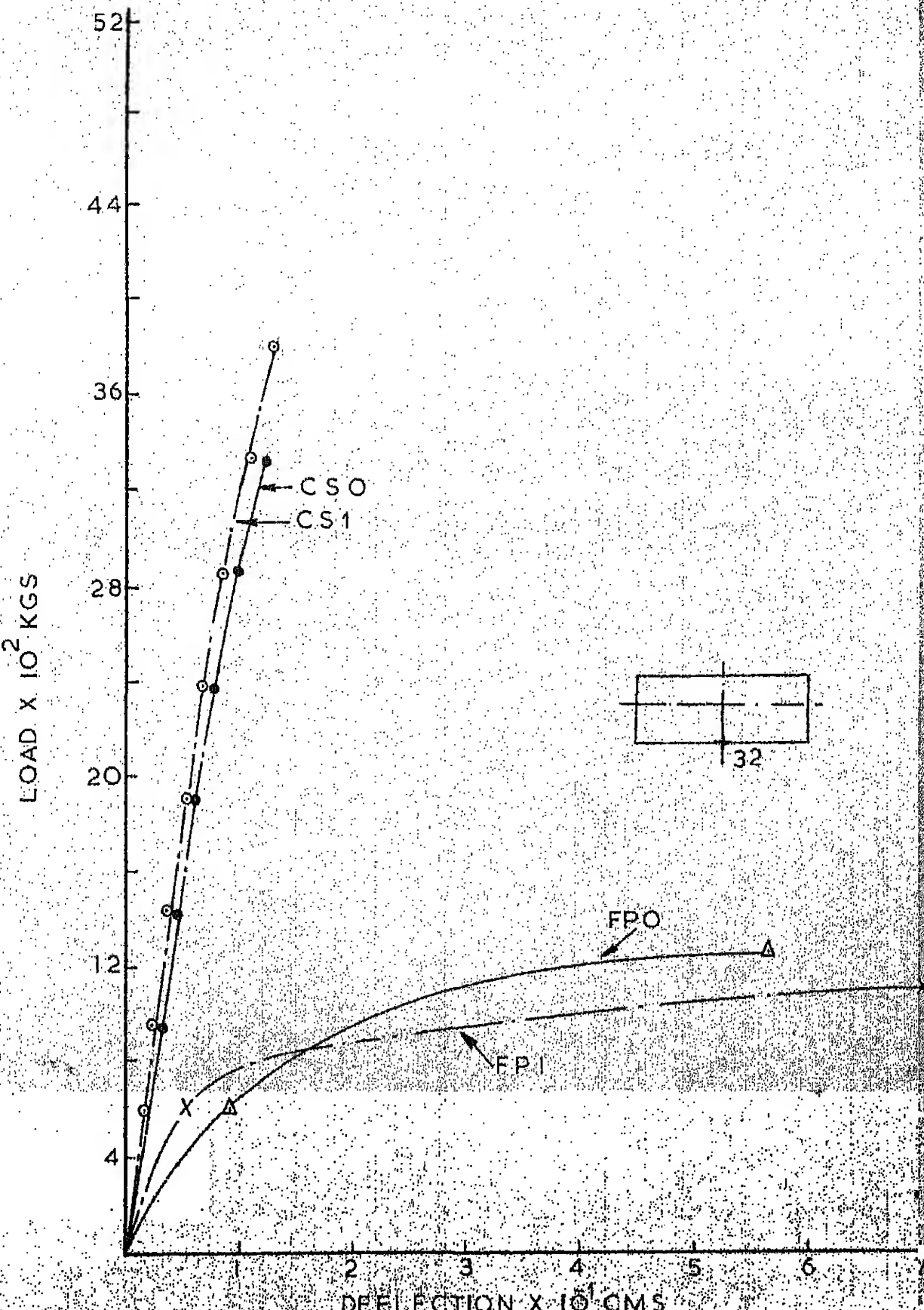

FIG. 4.14 COMPARATIVE STUDY OF IDENTICAL C-SHELL AND FOLDED PLATE

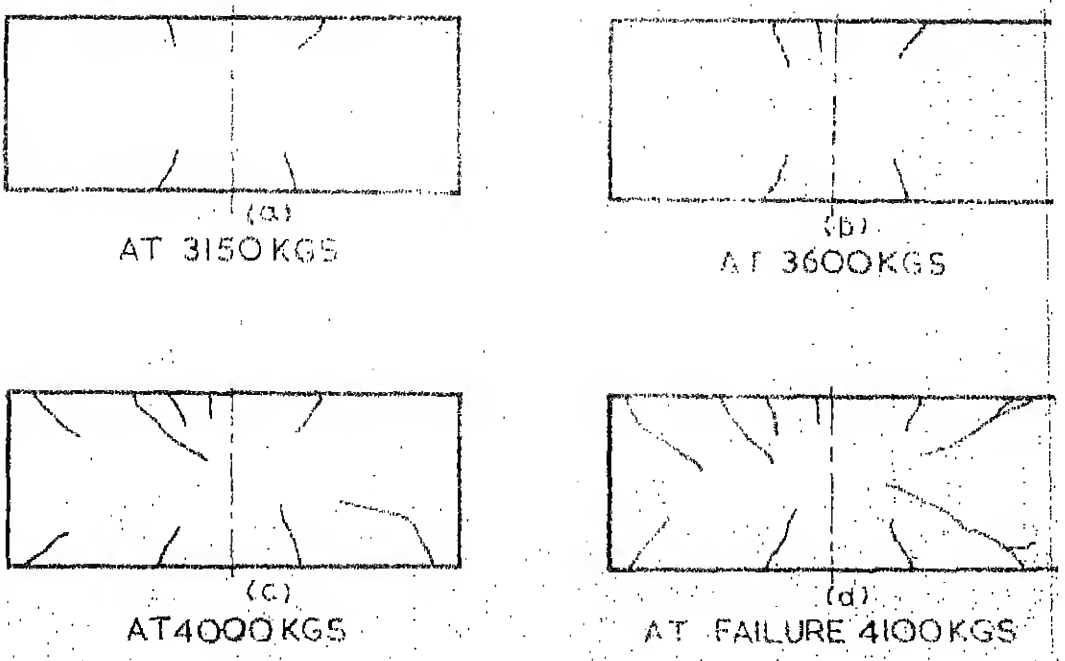

FIG. 4·15 CRACK PATTERN CSO

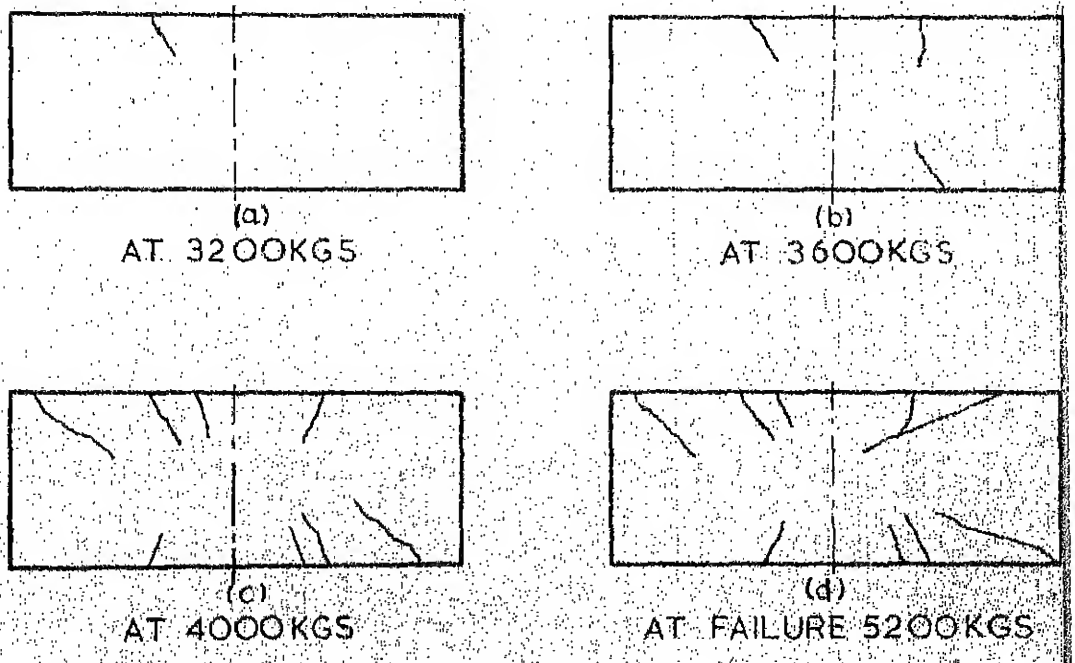

FIG. 4·16 CRACK PATTERN CS1

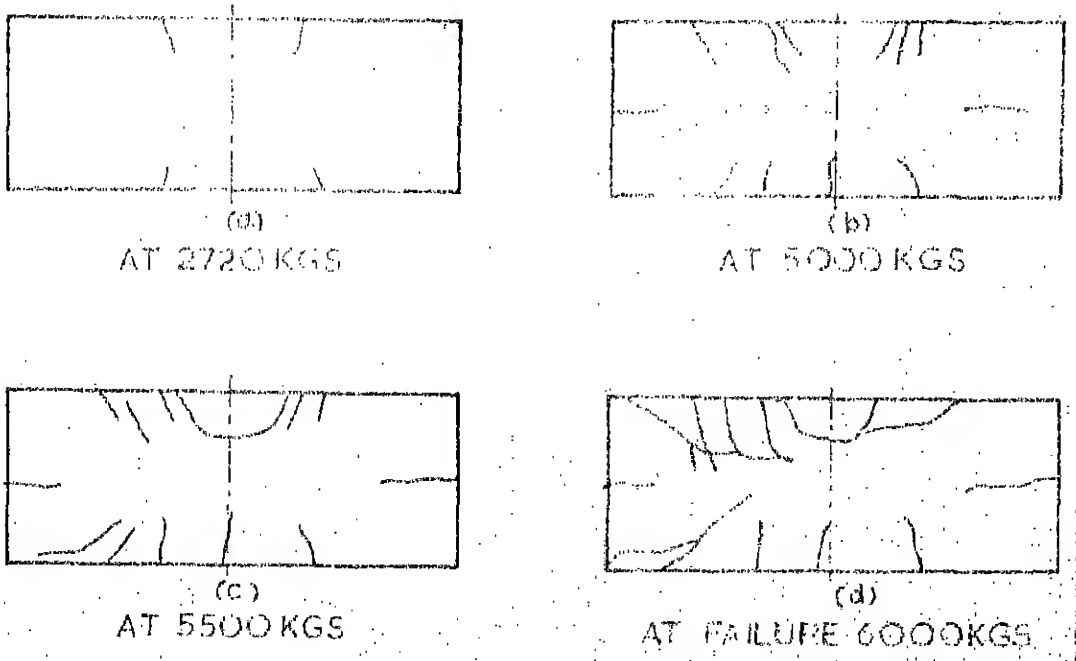

FIG. 4·17 CRACK PATTERN CS 3

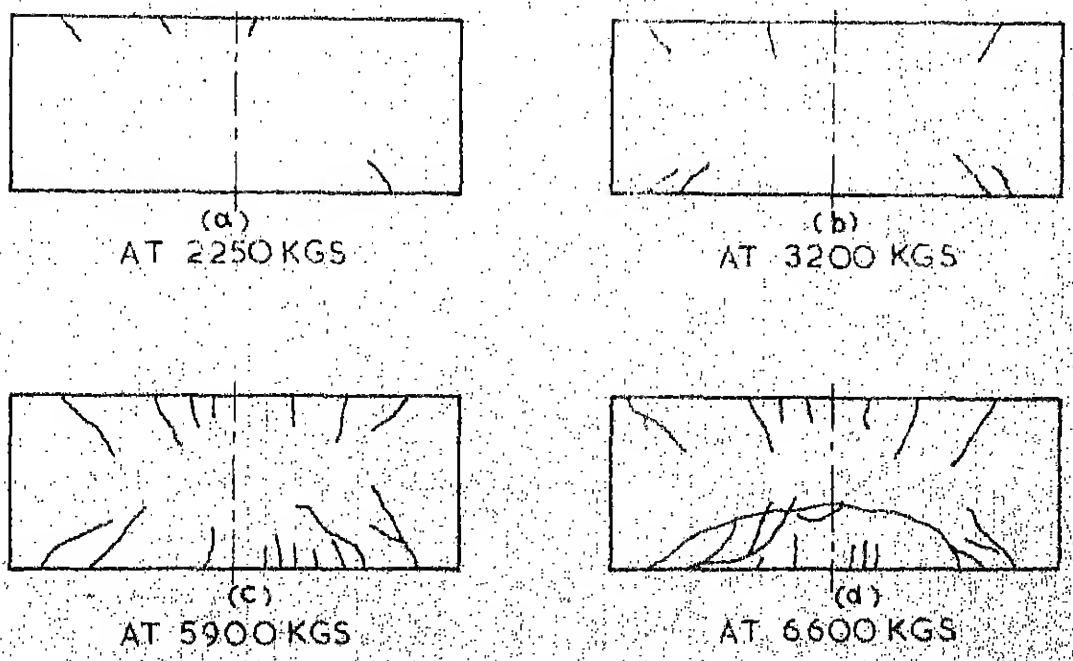

FIG. 4·18 CRACK PATTERN CS 5

CHAPTER V

CONCLUSIONS

(1) A cylindrical shell has a tendency to flatten out under two conditions:

(a) A shell with an edge beam with high flexural stiffness in the vertical plane and subjected to uniformly distributed vertical load.

(b) A shell with relatively less stiff edge beams but under some concentrated loads.

A need for transverse tie bar arises in such situations.

(2) Introduction of the tie bars at the springing level reduces the deflection of the shell. It was observed that the deflection is a function of the ratio of the chord-width to tie bar spacing. If t is ratio increases, the deflection decreases. If the spacing of the tie bar is kept nearly equal to the chord-width, this layout of the tie bars yields good results. As the spacing of the tie bars is decreased, the deflection does not get reduced proportionately, but gets reduced asymptotically.

(3) Not only the number of the tie bars, but also their position matters in the layout. The tie bars

near the support do not give the significant contribution.

(4) Horizontal force in a single tie bar spaced at 1.4 times of the chord width was of the order of 8% of the load acting on the specimen. Similarly, horizontal force in the single tie bar spaced nearly equal to the chord width was of the order of 6%. Knowing the load taken by the structure, the force in a single tie bar of the proposed layout can be found out. So, the layout of tie bars with the required area can be introduced.

(5) As the number of the tie bars increases, flexural and shear cracks develop in more number and their distribution is nearly uniform. The increase in the ultimate strength as the number of the tie bars is increased might be attributed to more number of cracks and their uniform distribution.

(6) The cracking load is not much influenced by the presence of the tie bars.

(7) The ultimate load increases as the number of the tie bars increases. The rate of the increase is rapid up to the chord-width/spacing ratio being 2, then the rate diminishes.

(8) Flexural strength of the shell is considerably higher than that of other roof structures. So, to make the full utilization of the flexural strength, shear failure should not occur. Care must be taken to provide sufficient shear reinforcement in the support zone.

(9) If the crack has formed at the springing level in the existing structure, that crack may be closed by introducing the tie bar at the crack location.

(10) The cylindrical shell is very stiff compared to the identical folded plate. The deflection in cylindrical shell is very much less compared to that in folded plate. The cylindrical shell with the thinner section in place of the folded plate, can be employed to do the same work done by the folded plate if form-work and skilled labour costs are not controlling factors.

REFERENCES

(1) Bouma, A.L., Van Riel, A.C., Van Koten, H., and Beranek, W.J., "Investigations of Models of Eleven Cylindrical Shells Made of Reinforced and Prestressed Concrete", Proceedings of the Symposium on Shell Research, Delft, Aug. 30 - Sept. 2, 1961, North Holland Publishing Company, Amsterdam 1961.

(2) Arya, A.S. and Agarwal, S.K., "Effect of Edge Beams on Stresses in Cylindrical Shells", Journal of the Institute of Engineers (India), Civil Engineering Division, March 1967, pp. 586 - 603.

(3) Arthur W. Hedgren Jr. and David P. Billington, "Mortar Model Test on a Cylindrical Shell of Varying Curvature and Thickness", Journal of American Concrete Institute, Feb. 1967, pp. 73 - 83.

(4) Kalra, M.L., "The Influence of Prestressing on Stresses in Single Shells", Indian Concrete Journal, Jan. 1967, pp. 32 - 36.

(5) ASCE, "Design of Cylindrical Concrete Shell Roofs", Manuals of Engineering Practice, No. 31, New York, 1952.

(6) Ramaswamy, G.S., "Design and Construction of Concrete Shell Roofs", McGraw-Hill Book Company, 1968.

(7) Indubhushan, P., "Behaviour of Reinforced and Prestressed Concrete Folded-Plates with Tie Bars", M.Tech. Thesis, January 1969, Dept. of Civil Engineering, Indian Institute of Technology, Kanpur.

APPENDIX A

A-1 : DESIGN OF SHELL

Working Stress Design

Balanced Design was applied to design the shell.

Data

The following properties were adopted to design the shell preliminarily.

Working Tensile Stress of Steel	t_s	= 1400 kgs/cm^2
Working Compressive Stress of Concrete	c_c	= 100 kgs/cm^2
Modulus of Elasticity of Steel	E_s	= 2. * 10^6 kgs/cm^2
Modulus of Elasticity of Concrete	E_c	= 2.7 * 10^5 kgs/cm^2
Effective Depth	d	= 20 cms

Calculations

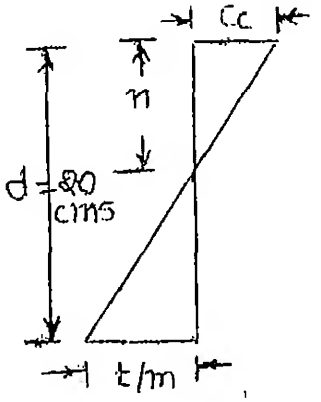

Stress Diagram

$$\text{Modular Ratio } m = \frac{E_s}{E_c}$$

$$= 20/2.7$$

$$= 7.4$$

From the stress diagram,

$$\frac{c}{t/m} = \frac{n}{d-n}$$

Substituting the values and solving,

$$\frac{100 \times 7.4}{1400} = \frac{n}{20-n}$$

$$n = 6.9 \text{ cms}$$

Compressive Area is obtained from geometry.

$$A_c = 47.6 \text{ sq.cms.}$$

Taking linear variation,

$$\text{Compressive force} = \frac{1}{2} \times c_c \times A_c$$

$$= \frac{1}{2} \times 100 \times 47.6$$

$$= 2380 \text{ kgs.}$$

For equilibrium,

$$\text{Tensile force} = \text{Compressive force}$$

$$A_s = 2380/1400$$

$$= 1.7 \text{ sq.cms.}$$

Taking 9.4 mm dia bar,

$$\text{Numbers of Bars} = \frac{1.7}{0.695}$$

$$= 2.44$$

Say, Two Bars of 9.4 mm in each edge beam are required.

A-2: DETERMINATION OF THE TIE BAR FORCE

The force is determined in the following steps.

(1) Ultimate-Moment by Whitney's theory is found out.

(2) The load to be acted upon the specimen is found out by equating external moment to ultimate-moment.

(3) Working load is evaluated by applying factor of safety.

(4) The horizontal thrust at the hinge of two-hinged arch is found out.

Data

$E_s = 2. * 10^6$ kgs/cm^2

$E_c = 2.7 * 10^5$ kgs/cm^2

$f_y = 2670$ kgs/cm^2

$f'_c = 275$ kgs/cm^2

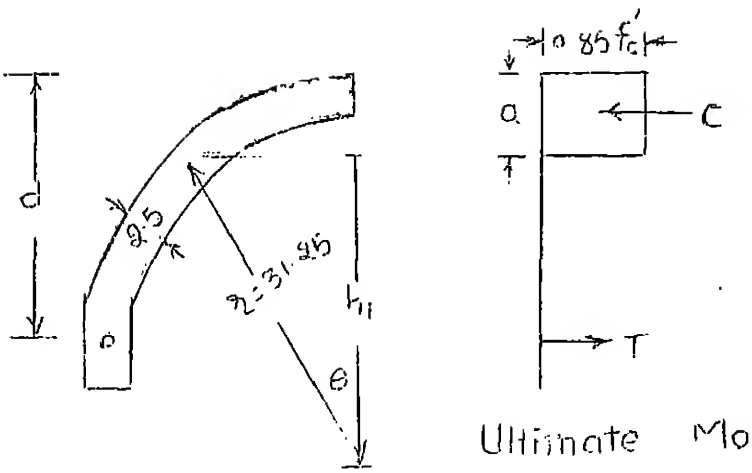

Ultimate Moment

Compressive force = Tensile Force

$(r\theta) \times t \times c_c$ = T (i)

Yielding of steel is assumed.

$T = A_s f_y$

$= 1.7 \times 2670$

$= 4540$ kgs

Taking (i) equation,

$(31.25 * \theta) * 2.5 * 0.85 * 275 = 4540$

$\theta = 0.246$ radians

$h_1 = r \cos \theta$

$= 30.3$ cms

Depth of stress block

$a = 32.5 - 30.3$

$= 2.2$ cms

Taking the centre of gravity of compressive area approximately at a/2 from top fibre.

$$\text{Ultimate Moment } M_u = T * (d - \frac{a}{2})$$

$$= 4540 * (20 - 1.1)$$

$$= 86{,}000 \text{ kgs-cms}$$

External Moment

The shell being loaded is shown in the following figure.

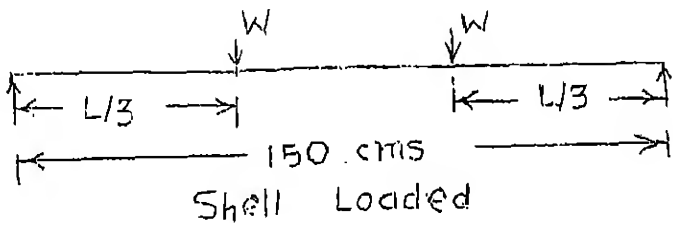

Shell Loaded

Maximum External Moment

$$= \frac{WL}{3} = 86{,}000 \text{ kgs-cms}$$

$$\therefore W = 1730 \text{ kgs}$$

Working Load

$$\text{at one point} = \frac{\text{Ultimate Load}}{\text{Factor of Safety}}$$

Say, factor of safety = 2

$$\text{Design Load} = \frac{1730}{2}$$

$$P = 865 \text{ kgs}$$

It is assumed that a point load equal to two points in magnitude acts at the centre of the shell. This assumption was considered to get rough idea about tie bar force at the centre.

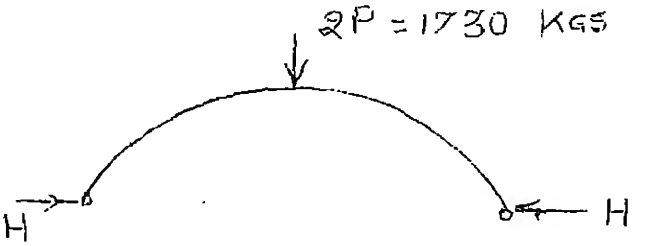

The horizontal thrust H can be found out. derivation is not shown,

$$H = 450 \text{ kgs}$$

Yield strength of high strength steel

$$= 14{,}800 \text{ kgs/cm}^2$$

Area of Steel = 0.0304 sq.cms.

However, high strength steel rod of 7 mm was adopted.

APPENDIX B

DETERMINATION OF FUNCTION FOR TIE FORCE AND ITS ORTHOGONALISATION

Determination of Function

Tie Bar Forces act as point forces along the span of the shell. The forces are expressed in Fourier Series. One example is illustrated for the case of one tie bar.

CS1: Cylindrical Shell with One Tie Bar

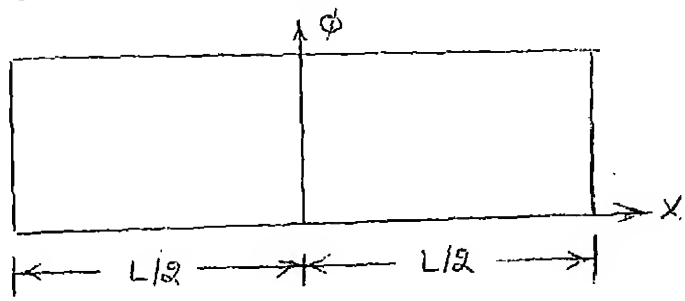

Say, the force in the tie bar is T. Say, the force is distributed over a length of L/20.

Introducing intensity 'p', the following equation can be written.

$$p \times \frac{L}{20} = T$$

$$\therefore \quad p = \frac{20\,T}{L}$$

$$f(x) = 0 \quad -\frac{L}{2} \leqslant x < -L/40$$

$$= p \quad -\frac{L}{40} < x < L/40$$

$$= 0 \quad -\frac{L}{40} < x \leqslant L/2$$

The function f(x) is represented in the following form

$$f(x) = a_o + \sum_{n=1}^{\infty} \left(a_n \cos \frac{n\pi x}{L} + b_n \sin \frac{n\pi x}{L}\right) \quad (B-1)$$

Function is even, hence b_n need not be calculated.

$$a_0 = \frac{1}{L} \int_{-L/2}^{L/2} [f(x)\, dx]$$

$$= \frac{1}{L} \int_{-L/40}^{L/40} [\, p dx \,]$$

$$= p/20$$

$$a_n = \frac{2}{L} \int_{-L/40}^{L/40} [\, p * \cos \frac{2n\pi x}{L}\, dx \,]$$

$$= \frac{2p}{n\pi} \sin \frac{n\pi}{20}$$

Substituting a_0 and a_n in (B-1), the function is obtained

$$f(x) = \frac{p}{20} + \frac{2p}{\pi} \sum_{n=1}^{\infty} \frac{1}{n} \sin \frac{n\pi}{20} * \cos \frac{n\pi x}{L} \qquad \text{(B-2)}$$

Substituting $p = \frac{20T}{L}$ in (B-2),

$$f(x) = \frac{T}{L} + \frac{40T}{L\pi} \sum_{n=1}^{\infty} \frac{1}{n} \sin \frac{n\pi}{20} * \cos \frac{n\pi x}{L}$$

Functions for various cases are following (derivations for other cases, not shown).

CS1: Shell with One Tie Bar

$$f(x) = \frac{T}{L} \left(1 + \frac{40}{\pi} \sum_{n=1}^{\infty} \frac{1}{n} \sin \frac{n\pi}{20} * \cos \frac{n\pi x}{L}\right) \qquad \text{(B-3)}$$

CS2: Shell with Two Tie Bars

$$f(x) = \frac{T}{L} \left[1.732 + \frac{34.64}{\pi} \sum_{n=1}^{\infty} \frac{1}{n} \left(\sin \frac{23\, n\pi}{60} - \sin \frac{17 n\pi}{60}\right) * \cos \frac{n\pi x}{L}\right. \qquad \text{(B-4)}$$

T in one Tie Bar

CS3: Shell with Three Tie Bars

$$f(x) = \frac{T}{L}\left[2 + \frac{20}{\pi}\sum_{n=1}^{\infty}\frac{1}{n}\left(\sin\frac{43n\pi}{60} - \sin\frac{37n\pi}{60} + 2\sin\frac{n\pi}{20}\right) * \cos\frac{n\pi x}{L}\right] \qquad \text{(B-5)}$$

T in Central Tie Bar

CS4: Shell with Four Tie Bars

$$f(x) = \frac{T}{L}\left[2.732 + \frac{20}{\pi}\sum_{n=1}^{\infty}\frac{1}{n}\left(\sin\frac{43n\pi}{60} - \sin\frac{37n\pi}{60} + 1.732\left(\sin\frac{23n\pi}{60} - \sin\frac{17n\pi}{60}\right)\right)* \cos\frac{n\pi x}{L}\right] \qquad \text{(B-6)}$$

T in Tie at $\frac{L}{6}$ from centre.

CS5: Shell with Five Tie Bars

$$f(x) = \frac{T}{L}\left[3.732 + \frac{20}{\pi}\sum_{n=1}^{\infty}\frac{1}{n}\left(\sin\frac{43n\pi}{60} - \sin\frac{37n\pi}{60} + 1.732\left(\sin\frac{23n\pi}{60} - \sin\frac{17n\pi}{60}\right) + 2\sin\frac{n\pi}{20}\right) * \cos\frac{n\pi x}{L}\right] \qquad \text{(B-7)}$$

T in Central Tie

Orthogonalisation

Equ. (3.6) is rewritten

$$[C][X] = [Y]$$

Say, first row is written as

$[\quad\quad]\cos\frac{\pi x}{L}$. Numerics as elements in brackets may be derived from boundary condition of horizontal thrust.

Example is illustrated for the case of one tie bar.

One Tie Bar

$$[\quad\quad]^* \cos\frac{\pi x}{L} = \frac{T}{L}\left(1 + \frac{40}{\pi}\sum_{n=1}^{\infty}\frac{1}{n}\sin\frac{n\pi}{20} * \cos\frac{n\pi x}{L}\right)$$

Multiplying both sides by $\cos\frac{\pi x}{L}$ and integrating them over the length

$$[\quad\quad]^* \int_{-L/2}^{L/2}\cos^2\frac{\pi x}{L}\,dx = \frac{T}{L}\left[\int_{-L/2}^{L/2}\cos\frac{\pi x}{L}\,dx + \frac{40}{\pi}\int_{-L/2}^{L/2}\left(\sum_{n=1}^{\infty}\sin\frac{n\pi}{20}\cos\frac{n\pi x}{L}\cos\frac{\pi x}{L}\,dx\right)\right]$$

If n = 1, then integral comes out to be L/2. In other values of n, integral vanishes.

$$\left[\qquad\right] * \frac{L}{2} = \frac{4T}{L\pi}\left[\frac{2}{\pi} + \frac{20}{\pi}\sin\frac{\pi}{20}\right]$$

$$\left[\qquad\right] = \frac{4T}{L\pi}\left[1 + 10\sin\frac{\pi}{20}\right] \qquad \text{(B-8)}$$

So, the right hand side of (B-8) becomes first row of $[Y]_{4x1}$.

Orthogonalised elements for various cases are following.

Orthogonalised Elements

$$CS1: \frac{4T}{L\pi} * \left[1 + 10\sin\frac{\pi}{20}\right] \qquad \text{(B-8)}$$

$$CS2: \frac{4T}{L\pi} * \left[1.732 + 8.66 * \left(\sin\frac{23\pi}{60} - \sin\frac{17\pi}{60}\right)\right] \qquad \text{(B-9)}$$

$$CS3: \frac{4T}{L\pi} * \left[2 + 5 * \left(\sin\frac{43\pi}{60} - \sin\frac{37\pi}{60} + 2\sin\frac{\pi}{20}\right)\right] \qquad \text{(B-10)}$$

$$CS4: \frac{4T}{L\pi} * \left[2.732 + 5 * \left\{\left(\sin\frac{43\pi}{60} - \sin\frac{37\pi}{60}\right) + 1.732\left(\sin\frac{23\pi}{60} - \sin\frac{17\pi}{60}\right)\right\}\right] \qquad \text{(B-11)}$$

$$CS5: \frac{4T}{I\Pi} * \left[3.732 + 5 * \left\{ \sin \frac{43\Pi}{60} - \sin \frac{37\Pi}{60} + \right. \right.$$

$$1.732 \left(\sin \frac{23\Pi}{60} - \sin \frac{17\Pi}{60} \right) +$$

$$\left. \left. + 2 \sin \frac{\Pi}{20} \right\} \right] \qquad (B-12)$$

APPENDIX C

CONVERSION OF LOADING

Uniform load in longitudinal direction is found out by virtual work concept. This uniform load is the line load acting at the ridge. The uniform load over the shell is obtained from the line load by simple statics

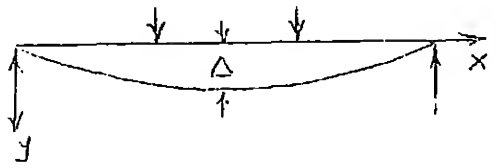

Fig. C-1
Loading at Ridge

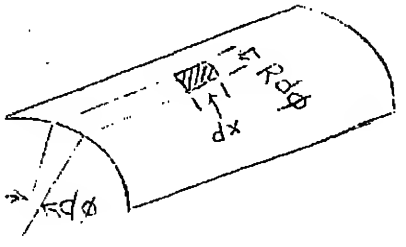

Fig. C-2
U.D.L. over Shell

Sine function for virtual displacement is assumed. Work done by two point loads,

$$= 2P * \Delta \sin \frac{\pi x}{L}$$

$$= 2P * \Delta \sin \frac{\pi L}{3L}$$

$$= 1.732P \qquad (C\text{-}1)$$

Work done by the uniform load over the shell,

$$dw = w_u * (dx\ Rd\theta) * y$$

Integrating,

$$W = \int_{-\phi_c}^{\phi_c} \int_{0}^{L} w_u R \Delta \sin \frac{\pi x}{L} \, dx \, d\phi$$

$$= 2 w_u \Delta \frac{L}{\pi} R * 2\phi_c \qquad (C-2)$$

Equating (C-1) and (C-2)

$$w_u = 1.36 \frac{P}{LR\phi_c} \qquad (C-3)$$

Substituting the values of R and ϕ_c in (C-3)

$$w_u = 0.04325 \frac{P}{L}$$

This loading is converted into Fourier Loading and its first term is considered.

$$\text{Loading in analysis} = \frac{4}{\pi} * 0.04325 \frac{P}{L}$$

APPENDIX D

TABLES FOR MULTIPLIERS AND COEFFICIENTS IN THE SCHORER THEORY (6)

Table D-1 Multipliers M_i in the Schorer Analysis $i=1,8$

Shell Action	Multiplier
$N_{x\phi}$	$-\frac{D\rho^4 L}{R^4 \pi} \cos\frac{\pi x}{L}$
Q_ϕ	$-\frac{D\rho^3}{R^3\sqrt{2}} \cos\frac{\pi x}{L}$
N_ϕ	$-\frac{D\rho^4}{R^3} \cos\frac{\pi x}{L}$
M_ϕ	$-\frac{D\rho^2}{R^2\sqrt{2}} \cos\frac{\pi x}{L}$
u	$-\frac{R}{L\sqrt{2}\rho^2} \cos\frac{\pi x}{L}$
w	$\cos\frac{\pi x}{L}$
v	$\frac{1}{\sqrt{2}\rho^2} \cos\frac{\pi x}{L}$
ϑ	$-\frac{1}{R} \cos\frac{\pi x}{L}$

where,

ρ = Aas - Jakobsen Parameter

$$\rho = \left(\frac{12}{L^4}\frac{R^6}{t^2}\right)^{1/8}$$

$$D = \frac{1}{12} Et^3$$

Table D-2 Coefficients $(B1, B2, B3, B4)_i$ $i=1,8$ in the Schorer Analysis (6)

Shell Action	B1	B2	B3	B4
$N_{x\phi}$	$+\beta_1$	$+\alpha_1$	$+\alpha_1$	$-\beta_1$
Q_ϕ	$(-\alpha_1+\beta_1)$	$(\alpha_1+\beta_1)$	$(\alpha_1+\beta_1)$	$(\beta_1-\alpha_1)$
N_ϕ	0	+1	0	-1
M_ϕ	+1	-1	-1	-1
u	-1	-1	+1	-1
w	+1	0	+1	0
v	$-(\alpha_1+\beta_1)$	$(\beta_1-\alpha_1)$	$(\beta_1-\alpha_1)$	$-(\alpha_1+\beta_1)$
ϑ	$-\alpha_1$	$+\beta_1$	$-\beta_1$	$+\alpha_1$

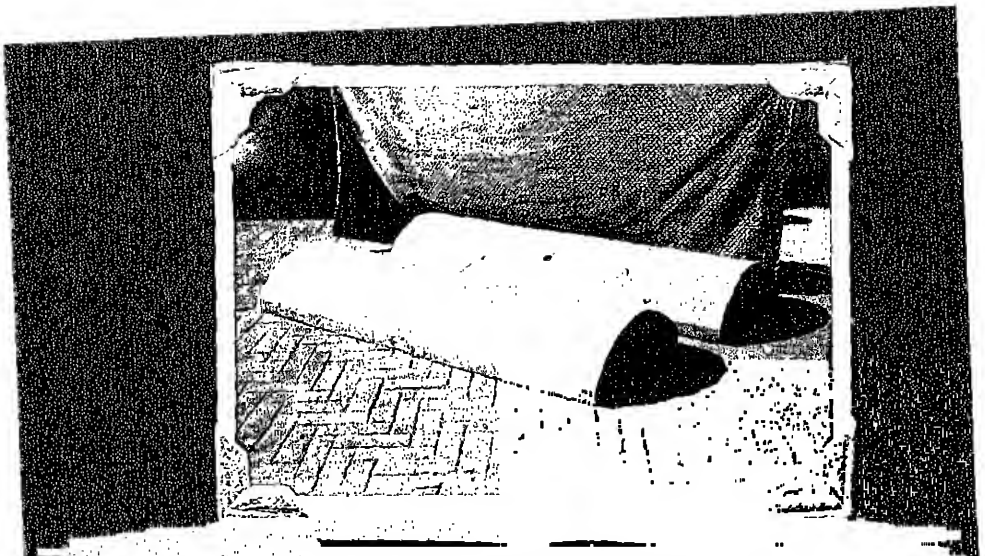

P:1 SPECIMEN VIEW

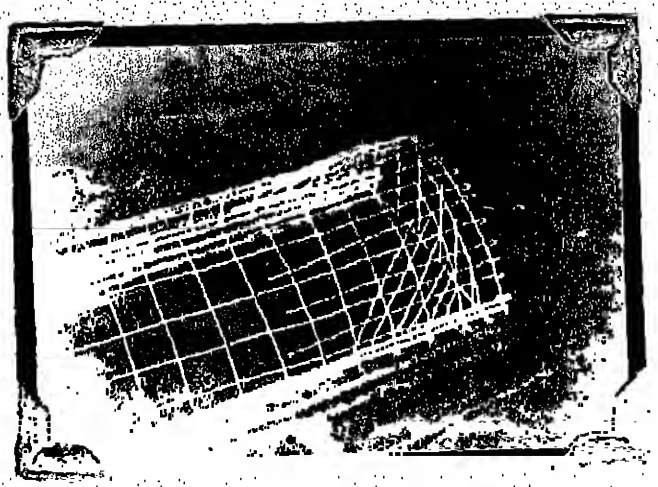

P:2 REINFORCEMENT IN SHELL

P:3 SET UP OF EXPERIMENT

CE-1969-M-MEH-BEH